Aus dem Experimental and Clinical Research Center

der Medizinischen Fakultät Charité - Universitätsmedizin Berlin und dem

Max-Delbrück-Center für Molekulare Medizin

DISSERTATION

Molekulare Mechanismen des Kolorektales Karzinom: MACC1 und das neuartige IER2-Gen

Molecular mechanisms of colorectal cancer: MACC1 and the novel IER2 gene

zur Erlangung des akademischen Grades
Doctor medicinae (Dr. med.)

vorgelegt der Medizinischen Fakultät
Charité – Universitätsmedizin Berlin

von

Miguel Enrique Alberto Vílchez
aus Caracas, Venezuela

Datum der Promotion: 23. März 2024

1 TABLE OF CONTENTS

TABLE OF FIGURES

TABLES

LIST OF ABBREVIATIONS

APC	Adenomatous polyposis coli
BAX	BCL2 associated X apoptosis regulator protein
BRAF	B-Raf proto-oncogene
CDC25A	M-phase inducer phosphatase 1
CDC4	Cell division control protein 4
CIMP	CpG island methylator phenotype
CIN	Chromosome instability
CK1	Casein kinase 1
CMS	Consensus molecular subtype
Co-IP	Co-Immunoprecipitation
CRC	Colorectal cancer
CREB	Cyclic AMP response element binding protein
CSC	Cancer stem cell
DFS	Disease-free survival
EGF	Epidermal growth factor
EMT	Epithelial-to-mesenchymal transition
ERK	Extracellular signal-regulated kinase
FAK	Focal adhesion kinase
FAP	Familial adenomatous polyposis

FDA	Federal Drug Administration
FGF	Fibroblast growth factor
FGFR	Fibroblast growth factor receptor
GAPDH	Glyceraldehyde 3-phosphate dehydrogenase
HCC	Hepatocellular Carcinoma
HDI	Human Development Index
HNPCC	Hereditary nonpolyposis colon cancer
HSF1	Heat shock factor 1
IEG	Immediate early gene
IER	Immediate early response
JNK	c-Jun N-terminal kinases
JUNB	Jun B proto-oncogene
KRAS	KRAS proto-oncogene
LOF	Loss-of-function
LOH	Loss-of-heterozygosity
MAPK	Mitogen activated protein kinase
MFS	Metastasis-free survival
MIN	Microsatellite instability pathway
MLH1	MutL homolog 1

mRNA	Messenger ribonucleic acid
MSH2	MutS homolog 2
MSI	Microsatellite instability
NF-κB	Nuclear factor kappa B
OPN	Osteopontin
OS	Overall survival
PDGF	Platelet-derived growth factor
PI3K	Phosphoinositide 3-kinase
Pip	Proline rich induced protein
PP2A	Protein phosphatase 2
PTEN	Phosphatase and tensin homolog
RPL32	Ribosomal protein L32
SASP	Senescence-associated secretory phenotype
SCNA	Somatic copy number alterations
SMAD4	SMAD family member 4
SRF	Serum-response factor
TGF	Transforming growth factor
TGFBR	Transforming growth factor-β receptor
TNM	Tumor-Node-Metastasis (classification)

TP53	Tumor protein 53
TPA	12-O-tetradecanoyl-phorbol-13-acetate
UICC	Union for International Cancer Control
WHO	World Health Organization

2 ABSTRACT

Background

Colorectal cancer (CRC) remains a clinical challenge as the third most common cause of cancer-related morbidity worldwide. The gene Metastasis-associated in colon cancer 1 (MACC1) is a key mediator of tumor progression and metastasis formation as well as a prognostic biomarker for CRC and more than 20 other solid cancer types. Higher MACC1 expression is associated with metachronous metastasis. Immediate Early Response 2 (IER2) is a novel player in the biology of metastasis. Previous studies have linked IER2 expression with enhanced metastatic capabilities, contributing to worse overall survival in different cancer entities. Concomitant upregulated mRNA expression of MACC1 and IER2 has been associated with worse overall survival in metastatic CRC patients, possibly identifying a population at high risk for metachronous metastatic disease. This dissertation addresses the question of a possible MACC1-driven IER2 regulation and the consequent metastasis formation.

Methods

We analyzed *in silico* mRNA expression profiles and predictive binding motifs for MACC1 and IER2. We made use of RT-qPCR, Western blot, co-Immunoprecipitation, clonogenic and proliferation assays to further understand the mechanisms behind a possible synergy among both genes. Furthermore, we used the CRISPR-Cas9 system for the creation of an IER2 knockout cell line.

Results

Cumulative survival for patients with a higher expression of IER2 and MACC1 genes was significantly worse. *In silico*, both a positive correlation between MACC1 and IER2 mRNA expression and a predicted SH3-mediated protein-protein interaction were found. Furthermore, overexpression of IER2 enhances colony formation in vitro, and silencing IER2 significantly hinders cellular proliferation.

Conclusion

MACC1, an established marker for metastatic disease, and IER2, a novel biomarker, may play an important synergetic role to confer enhanced proliferative and clone formation capabilities to cancer cells. From a clinical standpoint, the synergism between them undeniably translates into worst patient survival outcomes.

ZUSAMMENFASSUNG

Einleitung

Das kolorektales Karzinom bleibt eine klinische Herausforderung, da es weltweit die dritthäufigste Ursache für krebsbedingte Morbidität ist. Das Gen Metastasis-associated in colon cancer 1 (MACC1) ist ein wichtiger Vermittler der Tumorprogression und Metastasenbildung und ein prognostischer Biomarker für Darmkrebs und mehr als 20 andere solide Krebsarten. Eine höhere MACC1-Expression wird mit metachroner Metastasierung in Verbindung gebracht. Immediate Early Response 2 (IER2) ist ein neuer Akteur in der Biologie der Metastasierung. Frühere Studien haben die IER2-Expression mit einer erhöhten Metastasierungsfähigkeit in Verbindung gebracht, die bei verschiedenen Krebsarten zu einem schlechteren Gesamtüberleben beiträgt. Die gleichzeitige hochregulierte mRNA-Expression von MACC1 und IER2 wurde mit einer schlechteren Gesamtüberlebenszeit bei metastasierenden Darmkrebspatienten in Verbindung gebracht, was auf eine Risikopopulation für metachrone metastatische Erkrankungen hindeuten könnte. In dieser Dissertation soll die Frage nach einer möglichen MACC1-gesteuerten IER2-Regulierung und der daraus folgenden Metastasenbildung untersucht werden.

Methoden

Wir analysierten *in silico* mRNA-Expressionsprofile und prädiktive Bindungsmotive für MACC1 und IER2. Wir nutzten RT-qPCR, Western Blot, Co-Immunopräzipitation, klonogene- und Proliferationsassays, um die Mechanismen hinter einer möglichen Synergie zwischen beiden Genen besser zu verstehen. Außerdem verwendeten wir das CRISPR-Cas9-System zur Herstellung einer IER2-Knockout-Zelllinie.

Ergebnisse

Das kumulative Überleben von Patienten mit einer höheren Expression der Gene IER2 und MACC1 war signifikant schlechter. *In silico* wurde sowohl eine positive Korrelation zwischen der mRNA-Expression von MACC1 und IER2 als auch eine vorhergesagte SH3-vermittelte Protein-Protein-Interaktion gefunden. Darüber hinaus gewährleistet die

Überexpression von IER2 eine höhere *in vitro* Koloniebildungsfähigkeit, und das Silencing von IER2 hemmt die zelluläre Proliferation erheblich.

Fazit

MACC1, ein etablierter Marker für metastatische Erkrankungen, und IER2, ein neuartiger Biomarker, spielen möglicherweise eine wichtige synergetische Rolle, indem sie den Krebszellen eine erhöhte Fähigkeit zur Proliferation und Klonbildung verleihen. Aus klinischer Sicht führt die Synergie zwischen beiden zweifellos zu schlechteren Überlebensaussichten für die Patienten.

3 INTRODUCTION

3.1 Colorectal Cancer

Colorectal cancer (CRC) is among the most prevalent cancer diagnoses worldwide, hence it is a major cause of cancer-related morbidity and mortality. It is the third most commonly diagnosed cancer and within the top five leading causes of cancer deaths in the world in both men and women.[1] Important risk factors attached to CRC are advanced age, ethnicity, dietary choices, physical activity, obesity, smoking, and environmental factors.[2] As depicted in Figure 1, the majority of CRCs develop in patients without relevant family history (i.e. genetic predisposition) - this is also known as sporadic CRC. In contrast, a smaller subset of CRC cases can be directly attributed to monogenetic syndromes. Only about 8% of cases are linked to inheritable germline mutations.[2] The boundary between colon cancer and rectal cancer is determined by the anatomy. Distally of the sigmoid, the colon loses its mesentery to form the rectum. This happens approx. 16 cm before reaching the anus and serves as the limit between colon and rectal cancer. The rectum is divided into 3 parts depending on their distance to the anus: between 12 and 16 cm is the upper rectum, between 6 and <12 cm is the middle rectum, and <6 cm to the anus is the lower rectum. This is of importance because the respective sections feature different blood and lymphatic irrigation, and thus different routes for metastasis (Table 1).

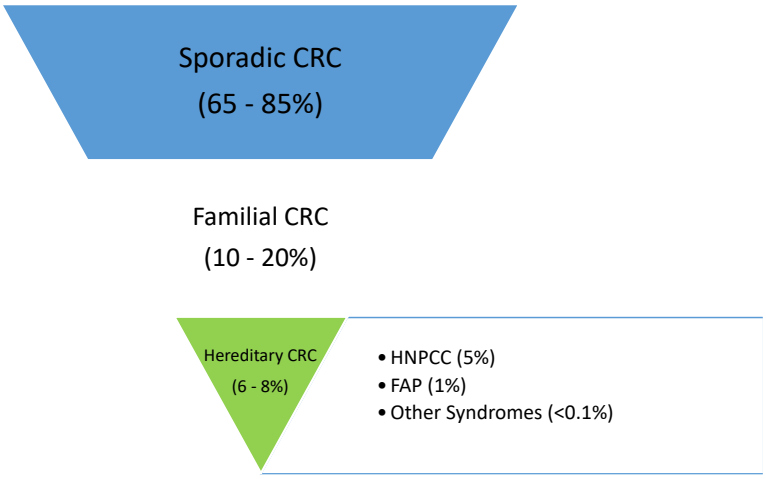

Figure 1

Graphical representation of proportion of CRC cases from different origins. Adapted from Feig *et al*.[2] HNPCC: hereditary nonpolyposis colon cancer, FAP: familial adenomatous polyposis.

Cancer		Distance to anus	Lymphatic metastasis	Hematogenous metastasis
Colon cancer		>16 cm	Mesenterial lymph nodes	V. portae: Liver V. cava inferior: Lung
Rectal cancer	Upper rectum	12 – 16 cm	Paraaortal lymph nodes	V. portae: Liver (also through V. rectalis superior and V. mesenterica inferior)
	Middle rectum	6 – <12 cm	Paraaortal and pelvic lymph nodes	
	Lower rectum	<6 cm	Paraaortal, pelvic and inguinal lymph nodes	V. cava inferior: Lung (also through Vv. rectalis media et inferior and V. iliaca interna)

Table 1 - Anatomical limits and metastatic paths in CRC.

3.1.1 Epidemiology

3.1.1.1 Latest statistics from World Health Organization

The latest epidemiologic cancer global report, GLOBOCAN 2020, recounted an estimated 1,931,590 diagnosed CRC cases (approx. 10% of all cancer entities – total: 19,292,789 cases)[1]. As depicted in Figure 2, CRC is in third place after lung and breast cancer. Mortality for the same period was reported at 953,173 people (approx. 9.4% - total: 9,958,133).[1] A more precise look into sex distribution shows 1-, 3- and 5-year prevalence in males of all ages worldwide to be between 12.1% and 12.6%. The same conditions for females apply, with a prevalence rate of 9.6 to 10%. Mortality risks differ just slightly. According to the same statistics, CRC maintains its ranking as the third cause of death in both sexes combined. In males, it rose to third place behind lung and liver cancers, as stomach malignancies dropped to fifth place. In females, CRC remains the third most common malignancy behind lung and breast cancer (Figures 3 and 4).

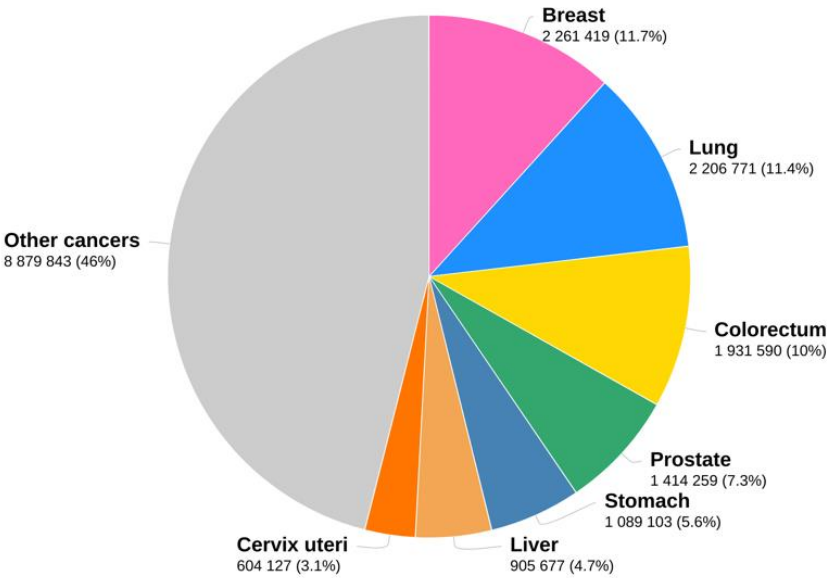

Figure 2

Estimated number of new cases in 2020, worldwide, all cancers, both sexes, all ages. Global Cancer Observatory (Globocan) 2020. Graph production: Globocan (http://gco.iarc.fr/). International Agency for Research on Cancer 2022.

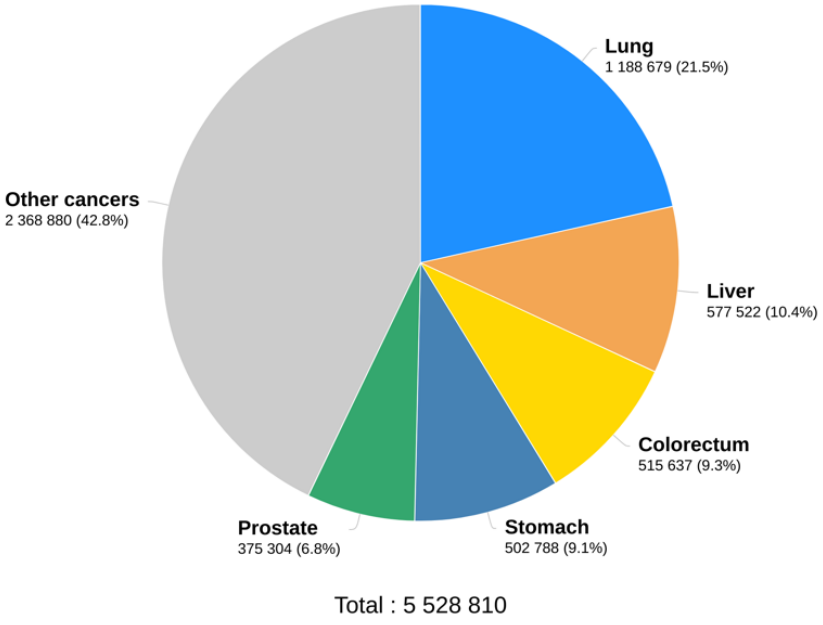

Figure 3

Estimated number of deaths in 2020, worldwide, all cancers, males, all ages. Global Cancer Observatory (Globocan) 2020. Graph production: Globocan (http://gco.iarc.fr/). International Agency for Research on Cancer 2022.

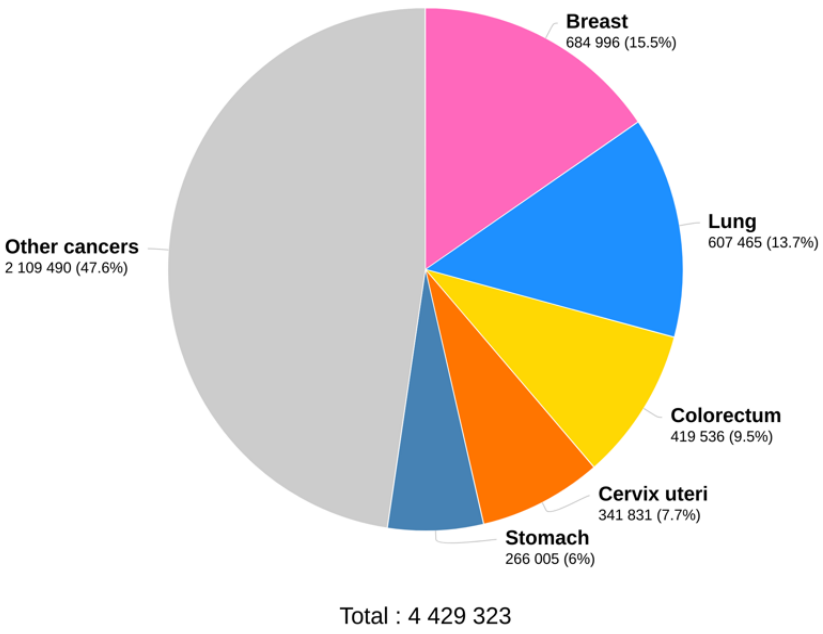

Figure 4

Estimated number of deaths in 2020, worldwide, all cancers, females, all ages. Global Cancer Observatory (Globocan) 2020. Graph production: Globocan (http://gco.iarc.fr/). International Agency for Research on Cancer 2022.

Incidence rates are about 3-fold higher in transitional versus transitioning countries (formerly known as developed versus undeveloped countries); however, with average case fatality higher in regions with lower Human Development Index (HDI), i.e., in transitioning countries, there is less variation in the mortality rates.[3] CRC is ultimately an indicator of socioeconomic development. The rises in incidence suggest the influence of dietary patterns, obesity, lifestyle, and environmental factors, whereas the declines in mortality seen in transitional countries reflect improvements in survival through the adoption of best practices in cancer treatment and management precisely in those countries that can afford such public health policies.[4] A clear example is depicted in Figure 5: observations over 3 decades have shown how the implementation of best medical practices (concerning systemic therapy, radiotherapy, and surgery), advances in

translational sciences, and targeted preventive screening have facilitated early-stage diagnosis, and thus, improved survival.

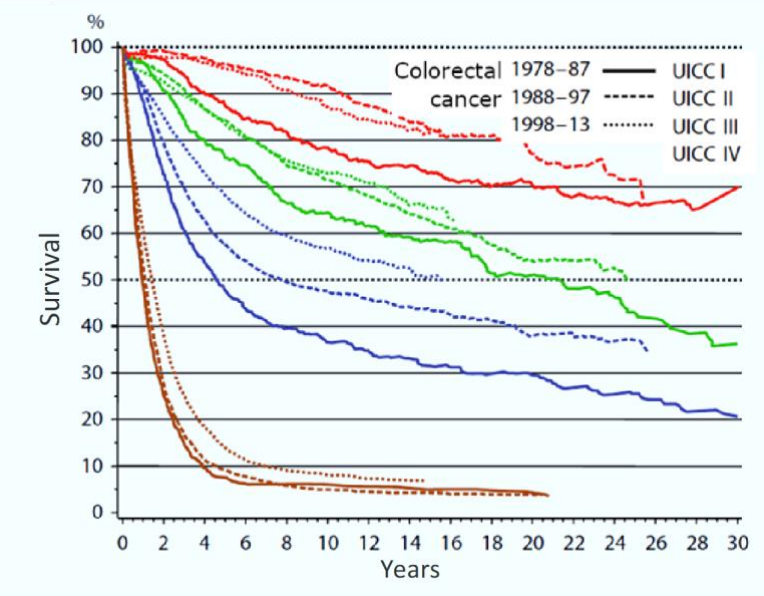

Figure 5

Union for International Cancer Control (UICC)-based stage regression at different time points in a German epidemiological study. Modified from: Hölzel e*t al*.[5]

The future for CRC patients is rather stygian from an epidemiological standpoint. According to the WHO, mortality rates worldwide are most likely to double until 2040 as the world moves towards higher HDI settings and occidental lifestyles are more readily adopted. Although Europe is following the same trend, as a continent with purely higher HDI countries and stronger public health systems, the projections only show a 10% increase. The mortality rate in Germany is expected to remain relatively the same (Figure 6).

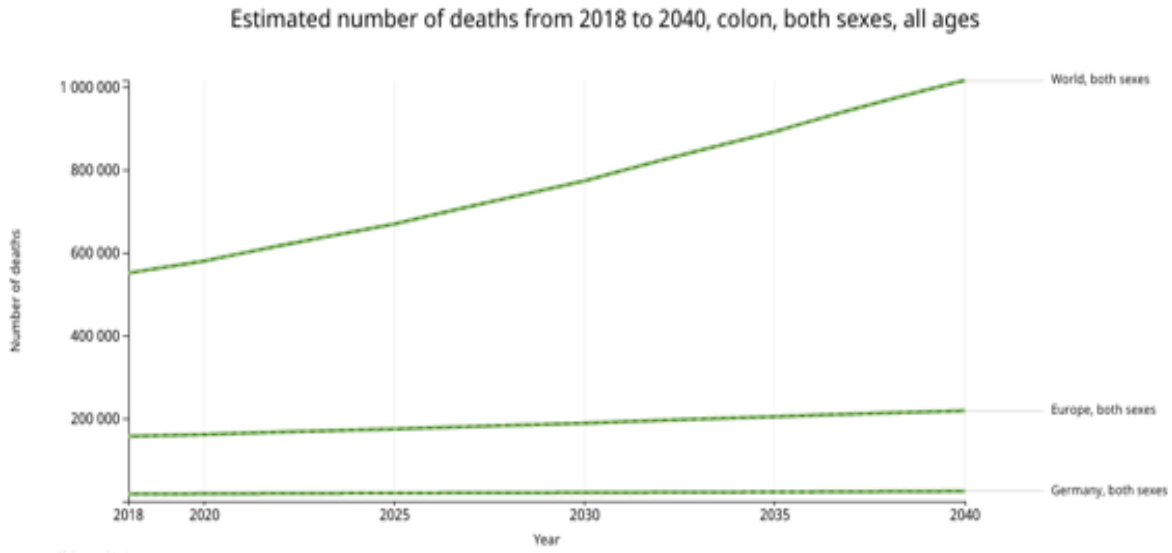

Figure 6

Estimations according to the WHO regarding deaths due to CRC for the next 20 years. Graphic depicts the world's mortality rate estimation as well as Europe's and Germany's. World Health Organization, Department of Information, Evidence and Research, mortality database (accessed in Feb 2020).

3.1.2 Risk and Protective Factors

The study of carcinogenesis and clinical outcomes over the years has identified the following risk factors to be of special relevance for CRC. Advanced age predisposes to the development of CRC, as the disease incidence increases steadily after 40 years of age and then exponentially after 50 years of age. Over 90% of newly diagnosed CRC cases, as well as CRC deaths, occur in patients over their fifth decade of life.[2] Ethnicity also plays an important role. In the United States, the disparity between African Americans and all other ethnic groups is significant. Both incidence and mortality are considerably higher when compared to their compatriots. When using the type of insurance as a surrogate for economic status, studies have shown concerning results. Using 5-year overall survival as a surrogate measure, CRC survival is about 30% higher among African American patients who are privately insured compared to uninsured fellow countrymen, confirming socioeconomic status as a major confounder.[2] The disparity is probably linked to important differences in access to screening associated with early disease prognosis, advanced treatment options and the most appropriate surgery.

Dietary patterns have also been studied as an important risk factor for CRC. Consumption of red and processed meat as well as animal fats, along with reduced intake of sources of natural fiber such as fruits and vegetables have been associated with a higher incidence of CRC. Specifically referring to a diet rich in fibers and whole grains, a continuous meta-analysis report by the World Cancer Research Fund found a 17% reduction in CRC risk per 90 g/day increase in consumption of whole grains. In the same report, a 100 g/day intake of red and processed meat was associated with a 12% higher risk of developing CRC. Furthermore, each 5 kg/m^2 increase in body mass index (BMI) is associated with a 5% increase in the risk of CRC.[6] Obesity, specifically central abdominal adiposity, might increase the risk of CRC due to a deficiency of short-chain fatty acid (SCFA)-producing bacteria and SCFA production in the intestine. SCFAs play an important role in maintaining metabolic homeostasis and a lower abundance of these acids has been associated with a higher risk of type 2 diabetes.[6–8] Through hitherto poorly understood mechanisms, increased circulating insulin and decreased peripheric insulin sensitivity, as well as changes in sex hormones and systemic inflammation have been shown to drive the risk for cancer.[6, 9] Regarding physical activity, the aforementioned report estimated a 19% risk reduction for colon cancer (not rectal) in high-level physically active individuals. The moderate consumption of alcohol seems to reduce the risk of CRC as well, provided that no more than 30 grams of ethanol, or 2 drinks, is imbibed per day.[2] Lastly, cigarette smoking promotes the formation of adenomatous polyps, which are particularly aggressive adenoma precursor lesions of CRC. Earlier onset of CRC has been reported in cigarette smokers.[2] Interestingly, patients subjected to cholecystectomy have an increased risk of developing CRC. This may be due to a higher burden of secondary bile acids due to a continuous flow of bile into the bowel. It is hypothesized that these secondary acids generate reactive oxygen and nitrogen species that cause DNA damage and promote resistance to apoptosis.[6, 10, 11] Further etiological considerations regarding the fecalome and metabolome in relation to CRC are reviewed by Song *et al*.[6]

3.1.3 Molecular Biology of CRC

Precision and translational medicine have been incredibly successful in prolonging patients' disease-free survival (DFS) and overall survival rates (OS). This success has

been granted by evolving treatment options towards a more personalized approach based on the characteristics of a patient's tumor, as opposed to the general populational tumor-node-metastasis (TNM) staging approach proposed by the Union for International Cancer Control (UICC). A key advancement in molecular biology has been the identification of prognostic and predictive biomarkers. A prognostic biomarker is used to assess the patient's overall cancer outcome regardless of any therapy the patient may have received. While a prognostic biomarker may help the clinician in deciding what treatment to administer, it will not predict the response to this treatment. Prognostic biomarkers may give information on recurrence after a given treatment or correlate with the duration of progression-free survival in patients with metastatic disease. Conversely, a biomarker with predictive value gives information on the effect of a therapeutic intervention on a patient. Hence, these can also be a target for therapy.[12] In CRC, few molecular biomarkers (including RAS and BRAF mutations as well as MSI and CIMP status) have been translated to patient care.[13]

Advancements in CRC genetics have made it possible for patients to receive personalized medical treatment by way of understanding the molecular changes that have shaped the development of target-specific pharmaceuticals and immune therapies. The adenoma/carcinoma progression sequence represents a widely acknowledged model of such deviations. CRC originates as the result of the accumulation of acquired genetic and epigenetic variations over time that will inevitably transform normal glandular epithelial cells into invasive adenocarcinomas.[14] This adenoma-to-carcinoma sequence, described first by Fearon and Vogelstein,[15] illustrates the transformational steps from normal epithelium into an adenoma (benign neoplasia), acquisition of invasive traits in epithelial-to-mesenchymal transition and eventually, metastatic cancer. To date, this model has been updated continuously. The detailed study of genetic and epigenetic alterations, as well as the further description of histological entities that also show malign progression patterns have helped this model maintain its validity.

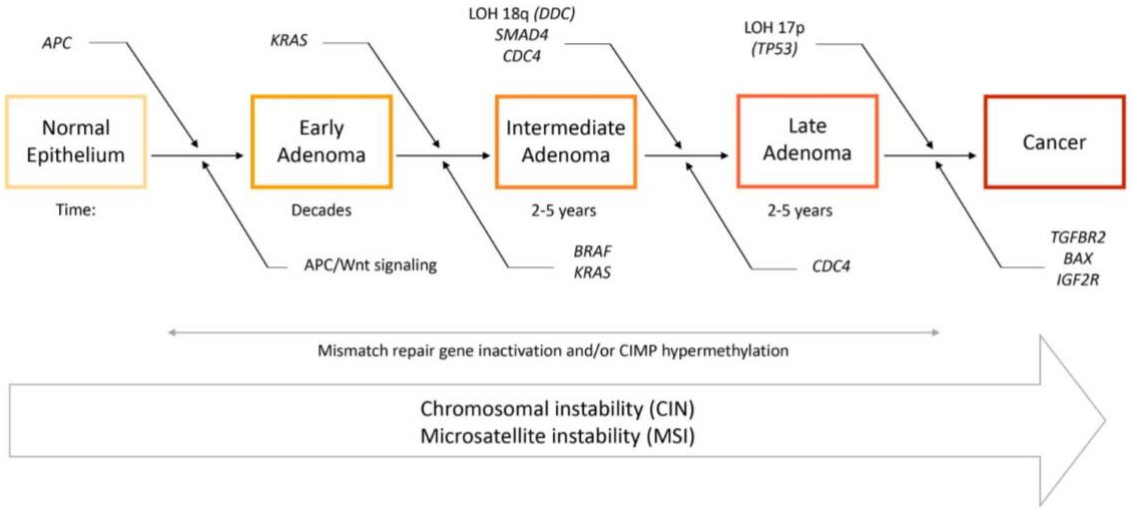

Figure 7

Adaptation of the adenoma-carcinoma sequence. An APC mutation is the first step towards transformation of normal epithelium to adenoma. Afterward, the CIN, MSI, and CIMP pathways work in parallel throughout the malignization process. CIMP: CpG island methylator phenotype, APC: adenomatous polyposis, KRAS: KRAS proto-oncogene GTPase; BRAF: BRAF Proto-oncogene serine/threonine kinase, TP53: tumor protein 53, LOH: loss of heterozygosity, TGFBR: transforming growth factor-β receptor; BAX: BCL2 associated X apoptosis regulator, CDC4: cell division control protein 4. Adapted from Nguyen *et al*.[16]

Hallmark features of colorectal carcinogenesis involve epigenomic instability. Originally, four kinds of epigenomic instabilities related to CRC were described: chromosomal instability (CIN), microsatellite instability pathway (MIN), CpG island methylator phenotype (CIMP) and global DNA hypomethylation.[16, 17] Classically, CIN has been described as the most common type of genomic instability in CRC. It can be found in approximately 85% of colorectal tumors, where breakage and improper annealing of chromosome fragments lead to loss of heterozygosity (LOH) mutations within tumor-suppressor genes such as APC, p53, or SMAD family member 4 (SMAD4).[16] Their respective gene products oppose malignant transformation physiologically, while their dysfunction contributes to chromosomal instability during replication.[18] APC, for example, is a protein that physiologically brakes Wnt/β-catenin signaling by degrading β-catenin via proteolysis and inhibiting its nuclear translocation. The most common mutation in CRC is a truncation of the gene region encoding the protein domains of APC that sequester β-catenin.[18] Another pathological mechanism at play involves the inactivation of genes required for the repair of base-base mismatches

in DNA named mismatch-repair genes. Inactivating germline mutations within these genes can be inherited, as in HNPCC, or acquired during abnormal DNA methylation events within tumors that silence genes encoding DNA mismatch-repair proteins.[18] The resulting deficiency in maintaining replicative DNA integrity is characterized as microsatellite instability. Here, tumor-suppressing genes, such as those encoding TGFBR2 and BAX are inactivated by deleterious, uncorrected point and frameshift mutations.[18, 19] Furthermore, epigenetic silencing of genes, mostly mediated by aberrant DNA methylation, serves as the third form of gene inactivation in CRC. Cancer cells have both a loss of global methylation and gain of methylation at the promoters of selected CpG islands, resulting in the silencing of an important number of genes, including tumor-suppressor genes.[20, 21] CpG islands are short regions containing a density of the CG sequence that map to promoter regions.[22] In CRC, aberrant methylation occurs similarly in known promoter regions and orphan (preceding non-annotated coding regions) CpG islands. This phenotype has been identified in approximately 35% of colorectal adenoma patients.[16] Interestingly, sporadic MSI CRC tumors are almost exclusively associated with CIMP-associated methylation, and therefore inactivation of MutL homolog 1 (MLH1), whereas familial MSI cases are generally caused by germline mutations in the MMR genes (MLH1 and MutS homolog 2 (MSH2)).[16, 23, 24]

In 2015, the CRC Subtyping Consortium (CRCSC) published a reviewed gene expression-based subtyping classification system for CRC.[13] It promised to be a more robust and detailed molecular classification system, in which 87% of tumors can be classified. The newly proposed taxonomy identifies four consensus molecular subtypes (CMSs): CMS1 (MSI immune), CMS2 (canonical), CMS3 (metabolic) and CMS4 (mesenchymal). The consortium concludes that the CMS1 group encompasses the majority of MSI tumors. These tumors are characterized by overexpressing proteins that hinder DNA mismatch repair, have a widespread hypermethylation status and are therapeutically relevant. Here are BRAF mutated tumors included. Contrariwise, CMS2, CMS3 and CMS4 displayed higher CIN. When looking into pathway activity, CMS1 is characterized by increased expression of immune evasion pathways and increased expression of genes associated with a diffuse immune infiltrate. CMS2 tumors showed strong upregulation of Wnt and MYC downstream targets as well as displaying epithelial

differentiation. In CMS3, enrichment for multiple metabolism signatures was found. Finally, CMS4 tumors evidenced an upregulation of genes involved in epithelial-to-mesenchymal transition (EMT) and signatures associated with the activation of transforming growth factor (TGF)-β signaling, angiogenesis, matrix remodeling pathways and the complement-mediated inflammatory system, as well as stromal infiltration, overexpression of extracellular matrix proteins and higher admixture with non-cancer cells.[13] The reason why such a revision was relevant is exemplified by the authors: when it comes to clinical decision-making at advanced stages, wild-type RAS tumors are considered to be a homogenous entity. These were, nevertheless, found across separate CMS groups with profound biological differences. This will inevitably translate into heterogeneous drug responses.[13] Table 2 reflects the aforementioned biological differences in gene expression-based molecular subtypes.

CMS1 MSI immune	CMS2 Canonical	CMS3 Metabolic	CMS4 Mesenchymal
14%	37%	13%	23%
MSI, CIMP high, hypermutation	SCNA high	Mixed MSI status, SCNA low, CIMP low	SCNA high
BRAF mutations		KRAS mutations	
Immune infiltration and activation	WNT and MYC activation	Metabolic deregulation	Stromal infiltration, TGF-B activation, angiogenesis
Worse survival after relapse			Worse relapse-free and OS

Table 2 - New proposed taxonomy of CRC.

MSI: Microsatellite Instability, CIMP: CpG island methylator phenotype, SCNA: Somatic copy number alterations, TFG-B: Transforming growth factor β, OS: overall survival. Adapted from Guinney *et al*.[13]

3.2 MACC1: a gene mediating metastasis in CRC

3.2.1 Advancement in metastasis research: MACC1

As published by a substantial number of groups, MACC1 (Fig. 8) has been established over the past decade as a key player in metastasis formation and tumor progression. Furthermore, it has consolidated its place as a biomarker for more than 20 solid cancer

types. These include, besides CRC, hepatocellular carcinoma (HCC), gastric, lung, cervical, ovarian, breast, and esophageal cancers, and glioblastomas.[25–27] To give a few examples, high MACC1 expression was demonstrated to predict postoperative recurrence of lung cancer.[28] When measured on CRC liver metastasis specimens, it is an independent prognostic factor of cancer recurrence,[29] and results after a multivariate analysis showed that HCC recurrence in the MACC1 overexpressing group after liver transplantation was significantly higher.[30] A direct relationship between high MACC1 expression in primary tumors, as well as their disposition towards the development of metachronous metastasis and poor patient survival has been extensively studied and published. According to a meta-analysis published by Wang *et al.*,[31] MACC1 overexpression is significantly associated with poorer OS and DFS in solid tumors. In CRC, this is most likely largely explained by the fact that tumors with UICC stages I – III (no distant metastasis) showed a higher MACC1 expression at the time of diagnosis with subsequent metachronous disease in comparison to those which did not metastasize and had lower MACC1 expression.[25]

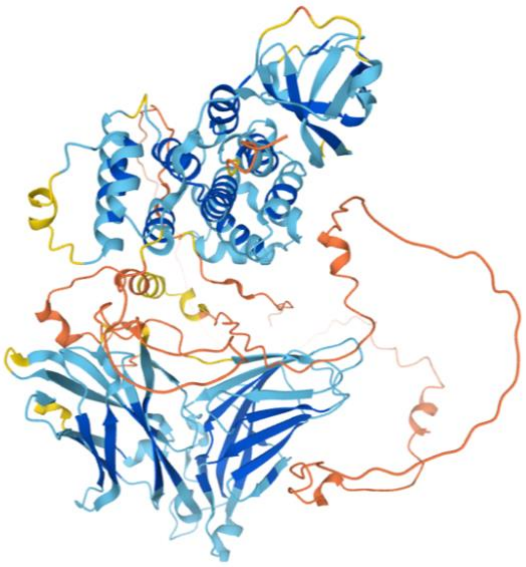

Figure 8

Most recent MACC1 protein structure prediction according to AlphaFold V2.0. Blue: Regions with pLDDT > 90 are expected to be modeled to high accuracy. Light blue: Regions with pLDDT between 70 and 90 are expected to be modeled well. Orange and yellow are values under 70 and 50 - these predictions are to be interpreted with caution or not interpreted. (Accessed on December 9th, 2021)

3.2.2 MACC1 and its role as a biomarker for metastatic colorectal cancer

The identification of MACC1 was directly related to an effort to find reliable biomarkers for metastatic disease. Ineffective treatment of metastasis leads to higher patient mortality. For colorectal cancer, the same applies, and so MACC1's importance in this disease has been gaining strength over the years. MACC1 levels in primary tumors were found to be significantly higher in patients who had developed metastases metachronously in comparison to those who had not, regardless of UICC stage. Higher MACC1 expression delivered higher mortality regardless of tumor stage, age, sex, tumor infiltration, nodal status, and lymphatic invasion.[32] The 5-year survival rate for patients with lower MACC1 expression in their tumors was 80%, compared to 15% for patients with low MACC1 expression.[32] Of note, when analyzing circulating transcripts harvested from patient plasma, an almost identical prognostication was possible. MACC1 levels were significantly higher in each disease stage of colon and rectal cancer compared with tumor-free volunteers. Furthermore, exceptionally higher levels were found in patients with newly diagnosed stage IV in comparison to those who had no metastases.[33] These findings qualify MACC1 for early detection of patients at risk in earlier disease stages, potentially even in liquid biopsy strategies.[25]

3.2.3 MACC1 and HGF-MET pathway regulation in colorectal cancer

Tyrosine phosphorylation and activation of tyrosine kinases are fundamental for cancer development, as they have a role to play in cell migration and proliferation.[34] Our group was able to associate a SH3 domain-mediated MACC1 interaction with the HGF-MET/Grb2–RAS-MAPK pathway.[32] Consequently, MACC1 and HGF-MET promotes increased motility and cell proliferation through scattering. Furthermore, MACC1 itself is upregulated by the MAPK pathway, which was "previously identified as a being essential for HGF-induced scattering",[32] working effectively as a positive feedback loop. This axis is then responsible for the sustainability of a proliferative and migratory signal. An immunohistopathological study[35] confirmed that MACC1 was expressed in important steps during the adenoma to carcinoma stages leading to CRC. Specifically, MACC1 was highly expressed independently of MET during the transition

between Tis (intramucosal carcinoma and/or high-grade dysplasia) and T1, and then subsequently T2. Later, parallel expression of MET and MACC1 was observed in liver metastasis in advanced CRC. This study implies that the MACC1/MET relationship may be reflected in the metastatic capacity of CRC.[35]

3.2.4 MACC1 mouse models

The first generation of mouse models for the study of MACC1 was carried out in 2016. Our group genetically engineered vil-MACC1 and vil-MACC1/APC^{Min} mouse models to better understand the tumor MACC1's role in the malign transformation of intestinal tissue. The results of Lemos *et al.*'s work demonstrated a novel axis with important therapeutic applications, namely the MACC1/Nanog/Oct4 pathway. This way MACC1 overexpression, in an APC-mutated background, significantly exacerbates tumor formation and progression.[36] Nanog confers immune surveillance evasion to cancer cells by a primarily CD59 mediated augmented resistance to lysis by cytotoxic T-Lymphocytes. Furthermore, it induces tumorigenicity by using a Akt pathway resulting in proliferation stimulation.[36, 37] The octamer-binding transcription factor (Oct4) has been under recent study as one of the main contributors to pluripotency and self-renewal of cancer stem cells (CSC). In addition, Oct4 and chemoresistance have been positively correlated in different cancer entities.[38, 39]

3.3 Immediate Early Response Genes

The cellular responses to immune-triggering events or cellular stress reactions are considered as immediate early response processes. These steer a specific group of genes that can respond very quickly to regulatory signals. After stimulation, mRNA transcripts occur in cells within minutes. Moreover, proteins required for their synthesis (i.e. transcription factors) are continuously synthesized within the cell and transduce the activation process immediately.[40, 41] Many of the members of the IER gene group are proto-oncogenes, as their expression has been observed to mediate cellular growth.[41]

Initiated by an extracellular signal, i.e., growth factors like platelet-derived growth factor (PDGF) and epidermal growth factor (EGF), expression of IER genes is mainly quick and transient. It does not require protein synthesis, and translational inhibitors have

no effect on their expression.[41] The combination of several mechanisms for rapid degradation and inactivation enables very transient signaling after gene activation. Other extracellular signals comprise mitogens, phorbol esters, immunological and neurological signals, and physical stress. Immediate early gene protein products are usually unstable and may be targeted for proteolytic degradation by the proteasome without prior ubiquitination. This has been observed for members of the FOS family.[42]

IEGs have on average shorter length than other genes (circa 19 kb), with significantly fewer exons and a high prevalence of TATA boxes and CpG islands.[41] According to Healy *et al.* [43], there is an enrichment for some specific transcription factor binding sites within regulatory regions of immediate early genes, including serum-response factor (SRF), nuclear factor kappa B (NF-κB), and cyclic AMP response element-binding protein (CREB) binding sites, which would suggest a consistent mechanism of transcription regulation. Important subfamilies, such as FOS and JUN, have been the focus of studies to prove them as oncogenes or to contribute to tumor progression after being subject to inappropriate expression or even mutations.

There are several pathways that activate the regulatory proteins necessary for IEG expression: RhoA-actin, extracellular signal-regulated kinase (ERK) and p38 mitogen-activated protein kinase (MAPK), and phosphoinositide 3-kinase (PI3K). These pathways lead to phosphorylation and activation of regulatory proteins such as transcription factor ELK1 and E twenty-six (ETS1/2), and also to regulatory factors such as SRF and Mediator complex.[41, 44]

3.3.1 IER2 and its features

In 1985 a group sought to identify genes that were expressed during the G0/G1 phase of the cell cycle.[45] In this attempt, a gene identified as *3CH92* was found to be overexpressed in the form of mRNA. Five years later, a report was published characterizing this gene and renaming it proline rich induced protein (pip92). It was then described as a “growth factor-inducible immediate-early gene.” The gene would encode a short-life unstable cytoplasmic protein. Throughout time, this gene has been renamed as 3CH92, ETR101, CHX1, pip92, and now IER2. Experiments in quiescent fibroblasts have shown that its mRNA accumulates rapidly and transiently after stimulation with

serum, PDGF, fibroblast growth factor (FGF), or 12-O-tetradecanoyl-phorbol-13-acetate (TPA). As a member of an immediate response gene family, transcription of IER2 is activated within 2 minutes of serum stimulation. Its peak level is reached by 10 minutes and is attenuated to low levels in 1 to 2 hours.[45, 46] During quiescence, IER2 is mainly cytoplasmic and after stimulation it is translocated to the nucleus. An up-to-date protein structure prediction is depicted below (Fig. 9).

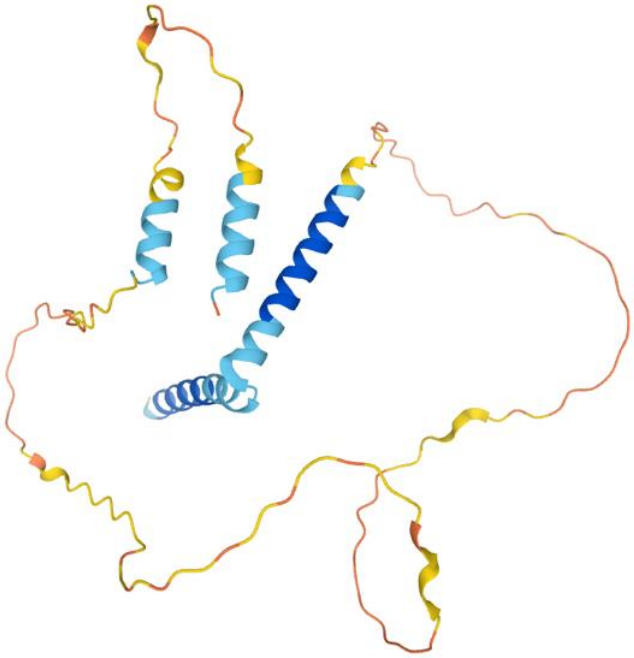

Figure 9

Most recent IER2 protein structure prediction according to AlphaFold V2.0. Blue: Regions with pLDDT > 90 are expected to be modelled to high accuracy. Light blue: Regions with pLDDT between 70 and 90 are expected to be modelled well. Orange and yellow are values under 70 and 50 - these predictions are to be interpreted with caution or not interpreted. (Accessed on December 9th, 2021)

3.3.2 IER2 and its role in cancer

As previously described, members of the immediate early response gene family are rapidly induced in quiescent cells upon proliferation- and migration-inducing stimuli. Gene expression of IER2 is differentially regulated under various growth conditions. p38 and JNK signaling elicit a particularly strong induction of IER gene members.[47] In 2012, Neeb *et al.* [48] described the correlation between IER2 expression and the metastatic phenotype in a wide range of human tumor entities. They successfully demonstrated three important characteristics of IER2. Firstly, IER2 was strongly upregulated in human

tumor tissue in comparison to its non-transformed counterpart. Tumor entities with the most prominent immunohistological staining signal were carcinomas of the esophagus, colorectum, thyroid, kidney, mammary glands, and cervix uteri. Secondly, the authors conclude that “there may be an upper threshold to IER2-induced motility”.[48] This conclusion was reached after observing that induction of IER2 expression does not invariably enhance cell motility, while selective knockdown reliably diminished motility after relief of contact inhibition in wounding assays. Additionally, increasing IER2 above endogenous levels in serum-induced post-quiescent fibroblasts did not improve their motility. Nevertheless, ectopic expression of IER2 promoted metastasis in *in vivo* experiments with otherwise poorly metastatic pancreatic tumor cells. Lastly, a clinical correlation between IER2 expression and overall survival of colorectal cancer patients was made.[48] This will be discussed further in a following subchapter.

At the molecular level, recent research has identified IER2 as an important player in various signaling pathways by regulating the substrate specificity of the protein phosphatase 2 (PP2A) holoenzyme. It not only interacts with PP2A but also its targets, thus enhancing phosphatase activity. IER2 binds to various B55 isoforms. These B subunits determine the substrate specificity, subcellular localization, and enzymatic activity of PP2A. Furthermore, IER2 binds to the PP2A substrates Heat shock factor 1 (HSF1) and M-phase inducer phosphatase 1 (CDC25A), consequently enhancing dephosphorylation of both proteins. A direct result of HSF1 dephosphorylation is induction of HSF1 transcriptional activity, whereas dephosphorylation of CDC25A causes dissociation from the widely cited 14-3-3 regulatory protein. Expression of IER2 causes dephosphorylation of T507 and dissociation of CDC25A from 14-3-3, thus enhancing CDC25A activity.[49] CDC25A, as a potential oncogene, is overexpressed in various human cancer entities. CDC25A is mainly localized in the nucleus, and it controls G1/S progression by inactivating Cyclin E/CDK2 and Cyclin D/CDK4-6 upon dephosphorylation.[50] As CDC25A is critical for both cell proliferation and apoptosis, its relationship to cancer becomes apparent.

Further studies have been conducted linking IER2 to oncological disease. IER2 has been identified as a regulator of cell-fibronectin adhesion, spreading and motility in two hepatocellular carcinoma (HCC) cell lines[51]. HCC is the fifth most commonly diagnosed

cancer worldwide and mortality is directly linked to metastasis. In this study, IER2 was demonstrated to induce HCC cell migration and invasion via regulation of cell-ECM adhesion and cell spreading. Ectopic overexpression of IER2 led to phosphorylation of focal adhesion kinase (FAK) at Y397, reduced phosphorylation of Src at its inhibitory site Y527, and paxillin phosphorylation,[52] all in response to fibronectin linking due to ITGB1 and ITGA5. This novel pathway may then be responsible for the metastatic potential of these two HCC cell lines.[51]

Most recently, IER2 has been associated with poor prognosis in melanoma patients. High levels of IER2 lead to the accumulation of an MDM2 isoform (MDM2-iso) that competes with the MDM2 full-length form (responsible for degradation of p53 by interacting with it), and increased activation of Akt and ERK1/2, which lead to stabilization of p53 and thus, expression of p21.[53] These mechanisms lead to a stochastic induction of senescence in melanoma cells. These cells express a distinctive senescence-associated secretory phenotype (SASP), where osteopontin (OPN) plays a fundamental role.[53] Furthermore, the association between IER2, p53/p21, and poor prognosis in melanoma patients suggests that IER2-induced senescence contributes to tumor progression.[53]

3.4 Aims of the dissertation

The identification of multiple effective agents including, but not limited to chemotherapy, immunotherapy, and radiotherapy for the treatment of CRC has brought a need for predictive markers to inform the selection of optimal treatment regimens for patients. This is particularly applicable to CRC due to the heterogeneity in response to, and the toxicity and cost of, medical treatments. The potential of genetic and epigenetic alterations to be effective predictive molecular markers has recently received considerable attention and has led to the use of some of these markers in the routine care of patients with CRC.[14] Here we have two potential markers, IER2 as a novel player in this field, and MACC1, that could lead us to better treatment strategies for our patients. In anticipation of such big questions, a more basic one must be answered first. Do MACC1 and IER2 work together or despite each other?

It is the aim of this thesis to answer this precise question. We have before us one confirmed (MACC1) and one potential (IER2) prognostic indicator for CRC outcome. The relationship between advanced stage (metastatic) CRC and poor overall survival has been widely studied. The association between metastasis and MACC1 has withstood a decade of research and still new connections are being found. From the clinical standpoint, CRC patients whose tumors expressed a higher MACC1 expression, have had earlier metastatic disease (worse metastasis-free survival [MFS]) and have died earlier (worse OS). It is our hypothesis that IER2 may have the same clinical effect. It is therefore the intention of the research presented to examine the possibility of a synergic action among MACC1 and IER2, or a separate but equally effective manner of promoting metastatic behavior in CRC cells due to overexpression of the IER2 gene. Research on this novel gene is still scarce and important questions remain unanswered.

There is careful consideration behind the methodology used throughout this research to answer questions regarding the mRNA and protein expression of MACC1 and IER2 in established CRC cell lines, as well as a possible correlation between the two genes of interest. Data retrieved from the Gene Expression Omnibus (GEO) data repository will be used for *in silico* analysis of this question. Co-Immunoprecipitation will be used to investigate a possible molecular interaction between the target proteins. Subsequently, the aim is to investigate the functional consequences of these expressions and interactions using proliferation and colony formation assays.

4 MATERIALS AND METHODS

4.1 Materials

4.1.1 Devices and Equipment

Item	Company
Cell culture incubator	Heraeus instruments (Hanau, Germany)
Countess™ automated cell counter	Invitrogen (Karlsruhe, Germany)
Cooling Centrifuge 5804 R	Eppendorf (Hamburg, Germany)
NanoDrop 1000	Thermo Fisher Scientific (Wilmington, USA)
Professional TRIO Thermocycler	Biometra (Jena, Germany)
Light Cycler® 480II	Roche Diagnostic (Mannheim, Germany)
Infinite F200 PRO	Tecan (Berlin, Germany)
Belly Dancer	Stovall Life Science (Greensboro, USA)
Trans-blot® Turbo™ Transfer System	BioRad Laboratories Inc. (Singapore)
Fuji Medical X-Ray Film	Minato (Tokyo, Japan)
ChemiDoc™ MP Imaging System	Bio-Rad (München, Germany)
Spectrafluor plus	Tecan (Berlin, Germany)
Vortex Genie 2™	Scientific Industries, Inc. (New York, USA)
Centrifuge 5810R	Eppendorf (Hamburg, Germany)
Incubator Shaker Series Excella E24	New Brunswick Scientific (New Jersey, USA)
IncuCyte® ZOOM	Essen Bioscience (Essen, Germany)

Table 3 - Devices and equipment.

4.1.2 Reagents, chemicals and resources

Reagents/Chemicals	Company
Fetal calf serum	PAA Laboratories (Cölbe, Germany)
DMEM medium	Thermo Fisher Scientific (Wilmington, USA)
Trypsin-EDTA	Thermo Fisher Scientific (Wilmington, USA)
Trypan-Blue	Invitrogen (Karlsruhe, Germany)
DMSO	Carl Roth (Karlsruhe, Germany)
MycoAlert™ Mycoplasma Detection Kit	Lonza (Basel, Switzerland)
Universal RNA purification kit	Roboklon (Berlin, Germany)
$MgCl_2$ (25 mM)	Applied Biosystems (Foster City, USA)
10 x PCR-buffer II	Invitrogen (Karlsruhe, Germany)
dNTPs	Biozym (Hessische Oldendorf, Germany)
RNase Inhibitor	Biozym (Hessische Oldendorf, Germany)
Random Hexamers	Biozym (Hessische Oldendorf, Germany)
MuLV Reverse Transcriptase	Biozym (Hessische Oldendorf, Germany)
Ethanol	Carl Roth (Karlsruhe, Germany)
GoTaq® qPCR Master Mix	Promega (Madison, USA)
PBS	PAA Laboratories (Cölbe, Germany)
BSA Standard	Pierce (Rockford, USA)
Pierce™ BCA Protein Assay Kit	Thermo Scientific (Wilmington, USA)
NuPAGE® LDS Sample Buffer	Invitrogen (Karlsruhe, Germany)
DTT	Sigma-Aldrich (Taufkirchen, Germany)

NuPAGE® 10% Bis-Tris Gel	Invitrogen (Karlsruhe, Germany)
Spectra™ Multicolor Broad Range Protein Ladder	Fermentas (Sankt Leon-Rot, Germany)
Ponceau S solution	Sigma-Aldrich (Taufkirchen, Germany)
Tween® 20	Carl Roth (Karlsruhe, Germany)
WesternBright™ ECL	Invitrogen (Karlsruhe, Germany)
PureYield™ Plasmid Miniprep System	Promega (Madison, USA)
Isopropanol	Carl Roth (Karlsruhe, Germany)
Opti-MEM medium	PAA Laboratories (Cölbe, Germany)
TransIT 2020	Invitrogen (Karlsruhe, Germany)
Silencer® Select Pre-designed siRNA	Ambion® (Carlsbad, USA)
Lipofectamine® RNAiMAX Reagent	Invitrogen (Karlsruhe, Germany)
G418	Sigma-Aldrich (Taufkirchen, Germany)
G-agarose beads	Alpha Diagnostic International Inc. (San Antonio, Texas)

Table 4 - Reagents, chemicals and resources.

4.1.3 Buffers

Buffer Name	Ingredients
1 x Phosphate Buffered Saline (PBS)	155 mM NaCl, 0.2 g, 1 mM KH2PO4, 3 mM Na2HPO4
1 x RIPA Buffer	50 mM TRIS pH 7.5 150 mM NaCl 1% Nonidet P-40 0.5 % sodium deoxycholate, Protease inhibitor

1 x Transfer Buffer	25 mM Tris-HCl pH 7.5, 200 mM Glycine, 0.1 % SDS, 20 % Methanol
1 x TBS-T	50 mM Tris-HCl pH 7.5, 150 mM NaCl, 0.1%, Tween®20
IP-lysis Buffer	20 mM Tris- HCl, pH 7.5, 150 mM NaCl, 0.1% NP40, 1 mM EDTA, 1% Triton X supplemented with complete protease inhibitor cocktail and phosphatase inhibitors from Roche Diagnostics (Risch, Switzerland)
Blocking Buffer	1 × TBS-T in 5 % skimmed milk
LB Medium	10 g/L Trypton, 5 g/L NaCl, 5 g/L Yeast extract
Mild Stripping Buffer	15 g/L Glycine, 1 g/L SDS, 10 ml Tween 20, pH2.2
Bovine serum albumin (5%)	5g in 100ml TBS-T
LDS Buffer	Thermo Fisher Scientific (Waltham, Massachusetts)

Table 5 - Buffers.

4.1.4 Antibodies

Primary antibody and concentration	Dilution	Manufacturer
Anti-human MACC1 (Rabbit, polyclonal IgG)	1:1,500 in 5% BSA in TBS-T	Sigma Aldrich (München, Germany)
Anti-β-actin 1mg/ml (Mouse, monoclonal IgG)	1:20,000 in 5% BSA in TBS-T	Thermo Scientific (Wilmington, USA)
Anti-IER2 1mg/ml (Rabbit, polyclonal)	1:1,000 in 5% BSA in TBS-T	Sigma Aldrich (München, Germany)

Anti-V5 (Mouse, monoclonal IgG)	1:1,000 in 5% BSA in TBS-T	Thermo Scientific (Wilmington, USA)
Secondary antibody	**Dilution**	**Manufacturer**
Anti-Rabbit-HRP	1:10,000 in TBS-T	Promega Corporations (Madison, USA)
Anti-mouse-IgG-HRP 0.8mg/ml	1:30,000 in TBS-T	Pierce - Thermo Scientific (Wilmington, USA)

Table 6 - Antibodies.

4.1.5 Software

Software	Remark
Magellan 7	Evaluation of photometric measurements and luminescence measurements
GraphPad Prism v6.0, v7.0, v9.0	Graphs, statistical analysis
Microsoft Office 2010/2019	Data calculation, manuscript preparation

Table 7 - Software.

4.2 Methods

4.2.1 Cell culture

Cell culture conditions were maintained to internal laboratory standards. Human CRC cell lines SW480, SW620, as well as HCT116, RKO and DLD1, all originally from the American Type Culture Collection, were grown in either Dulbecco's modified Eagle's medium (DMEM) or Roswell Park Memorial Institute (RPMI) medium (both Thermo Fischer Scientific) supplemented with 10% fetal bovine serum (FBS, Thermo Fisher Scientific). The generation of stable SW480 cell lines, with or without ectopic MACC1 expression (SW480/MACC1 and SW480/ev, respectively), has been described previously.[32] The establishment of SW620 clones with short hairpin (shRNA) and its control (SW620/shMACC1 and SW620/shCtrl, respectively) has been described

previously.[32] The HCT116/IER2 and HCT116/ev cell lines (with and without IER2 ectopic expression) were generously provided by Prof. Jonathan Sleeman from the University of Heidelberg. The genetic knockout of IER2 in the SW620 cell line was performed with the CRISPR/Cas9 technology following published protocols, resulting in a guide RNA-mediated shift in the reading frame of IER2 (gRNA-1: TATCACTCCCGCATGCAGCG; gRNA-2: CGTCGTTTGCGGCTGACT; SW620/ko-IER2) and the control cell line without the transfection of guide RNA (SW620/ko-ctrl). Alterations in the IER2-coding region of single-cell sorted clones were confirmed by LGC Genomics. All cells were maintained at 37°C in a humidified incubator with 5% CO_2. Regular corroboration of mycoplasma contamination-free culture was carried out using the MycoAlert Mycoplasma detection kit (Lonza). Routine cell culture passaging was carried out at around 80% confluence or at the latest every 3 - 4 days, depending on the cell line. For this process, Trypsin-EDTA (Thermo Fischer Scientific), PBS, and fresh medium were used. For continuous positive selection of MACC1-overexpressing cells, G418 (Roche Applied Sciences) was used.

4.2.2 Cell counting

Cell counting was carried out cautiously to maintain comparable flask density after seeding the cells. For the determination of cell numbers following growth to 80% confluence, the cells were detached from the bottom of the flask or dish using Trypsin-EDTA (Thermo Fischer Scientific) after being washed once with PBS at room temperature. Trypsinization was halted after a five-minute incubation with media supplemented with 10% (v/v) FBS. Using a vacuum pipettor, the cells were washed off the vessel and carefully mixed into a homogenous single cell suspension. 10 µl were taken and mixed with 10 µl Trypan blue to count living cells. For determination of the concentration of cells in the suspension, 10 µl of the resulting mixture were inserted into a counting slide for analysis under an automated cell counter. The Trypan blue dye is not absorbed by vital cells, which greatly improves their visibility against a dark blue background within the counting chamber. Further dilutions, as required by the respective experiment, were calculated based on the cell concentration and were accordingly seeded in new flasks.

4.2.3 RNA extraction and RT-qPCR

For RT-qPCR quantifications, laboratory standards were upheld. In 6-well plates, 300,000 cells were plated and grown until 80% confluence was reached. Total RNA was isolated using the Universal RNA Purification Kit (Roboklon, Germany) according to the manufacturer's instructions. 50 ng of purified RNA were reverse transcribed in a 20 µl total reaction mixture with 1.25 µM random hexamers, 1 × RT-buffer/dNTP mixture of 1 mM each, 1 U/µl RNase inhibitor and 10 U/µl MuMLV reverse transcriptase (all Biozym). Reaction occurred at 30°C for 10 min, at 50°C for 40 min, at 99°C for 5 min and there was subsequent cooling at 4°C (Biometra). The generated cDNA was subjected to gene specific qPCR using the HotStart DNA Master SYBR Green I Kit (Biozym) according to the manufacturer's instructions. The following gene-specific primer sets were used: MACC1 fwd: 5′-TTC TTT TGA TTC CTC CGG TGA-3′; MACC1 rev: 5′-ACT CTG ATG GGC ATG TGC TG-3′; IER2 fwd: 5′-AGT GCA GAA AGA GGC ACA GC-3′; IER2 rev: 5′-ACC TTG GCC GAG AGG TAG AG-3′ RPII fwd: 5′-GAA GAT GGT GGG ATT TC-3′; RPII rev: 5′-GAA GGT GAA GGT CGG AGT-3′; G6PDH fwd: 5′-ATC GAC CAC TAC CTG GGC AA-3′; and G6PDH rev: 5′-TTC TGC ATC ACG TCC CGG A-3′. Each PCR reaction was performed in a total volume of 10 µl in a LightCycler 480 system (Roche). After initial denaturation at 95°C, the amplification occurred within 40 cycles of denaturation (5 s; 95°C) and a combined primer annealing and elongation step (45 s; 60°C). Data analysis was performed with LightCycler 480 Software release 1.5.0 SP3 (Roche Diagnostics). Mean values were calculated from duplicates. Each mean value of the expressed gene was normalized to the respective mean amount of G6PDH or RPII (taken as housekeeping genes). The results were obtained from at least three independent experiments.

4.2.4 Protein extraction and Western Blot

Cells were grown in 6-well plates and - after achieving the desired confluence - were washed with 1x PBS. Cells were lysed with RIPA buffer for 30 min on ice. Protein concentration was quantified with Bicinchoninic Acid Protein Assay Reagent (Thermo Fisher Scientific) according to the manufacturer's instructions. Lysates of equal protein concentration were separated by SDS-PAGE and transferred to PVDF membranes

(Biorad). Membranes were blocked for 1 h at room temperature with 5% non-fat dry milk reconstituted in TBS-T buffer. Membranes were then incubated overnight at 4°C with MACC1 antibody (Sigma-Aldrich, dilution 1:1,000 BSA 5%), IER2 antibody (Sigma-Aldrich, dilution 1:1,000), β-actin antibody (Sigma-Aldrich, dilution 1:10,000) or V5 antibody (Thermo Scientific, dilution 1:1,000), followed by washing with TBS-T before final incubation for 1 h at room temperature with HRP-conjugated anti-rabbit IgG (Promega, dilution 1:20,000) or anti-mouse IgG (Thermo Fisher Scientific, dilution 1:10,000). Antibody-protein complexes were visualized with WesternBright ECL substrate (Invitrogen) and subsequent exposure to Fuji Medical X-Ray Film (Fujifilm). Western blot for β-actin or V5-tag served as the protein loading control. The results were obtained from at least three independent experiments.

4.2.5 Co-Immunoprecipitation

For Co-Immunoprecipitation (Co-IP), five million cells were seeded in 10 cm cell culture dishes and incubated for 24 h to form a cell monolayer. Cell monolayers were then washed once with 1x PBS and scratched off in 500 µl of ice-cold IP-lysis buffer and transferred to sterile reaction tubes. Cells were lysed for 30 min with intermittend vortexing at low intensity. Proteinous whole cell lysate was obtained by centrifuging for 45 min at 14,000 rpm at 4°C. The supernatants were collected and divided in 2 mg protein lysate aliquots. To precipitate the protein of interest, 2 µg of the respective target antibody was added to the lysate aliquot to be incubated overnight at 4°C on a rotational shaker. The protein-antibody complexes were absorbed to 20 µl of G-agarose beads for 4 h at 4°C on a rotational shaker. Subsequently, G-agarose beads were precipitated by centrifugation at 500 rpm for 45 min at 4°C, Supernatants were discarded, and beads were washed five times with 200 µl of IP-lysis buffer, followed by centrifugation at 2,500 rpm for 5 min at 4°C. After the final washing step, protein complexes were eluted with 30 µl of DTT-supplemented LDS buffer (1:10) at 99°C for 10 min. Following another spin at 2,500 rpm for 5 min at 4°C, 20 µl of supernatant were used for Western blotting using the method described above.

4.2.6 Proliferation Assay

Twenty thousand cells were plated in 96-well plates after passaging using the aforementioned technique. Each cell line was plated in technical duplicates. The corresponding medium was added. Plates were then placed in the IncuCyte® ZOOM. The hardware where the plates are mounted was maintained at 37°C in a humidified incubator with 5% CO_2. Using the manufacturer's software, the system was calibrated to take images every 2 h. After 96 h, the assay was halted, and the data points were collected. The software allows for quantification of cell confluence. The results were obtained from at least three independent experiments.

4.2.7 Colony Formation Assay

Four hundred cells were plated in 6-well plates after using the technique mentioned above. Each cell line was plated in technical duplicates. Cells were left to grow for 7 to 10 days at 37°C in a humidified incubator with 5% CO_2. A staining solution was used to enhance the visualization of the colonies that were formed. The colonies were stained for 1 h at room temperature. Afterward, plates were carefully rinsed off with water. Images of the wells were taken using a chemical imager. A template was made using the manufacturer’s software. Using transillumination with white light, images of the plates were made. These were then converted and analyzed using the open license software ImageJ. The open license plugin Colony Counter was used to count the colonies that were formed. This software also allows for colony area quantification. Threshold parameters were adjusted to include all visible colonies in the scanned area. The results were obtained from at least three independent experiments.

4.2.8 Survival analysis

Survival data described using Kaplan-Meier plots were calculated by bioinformatician Dr. Marc Osterland, PhD of the Stein Group in the Max-Delbrück-Center for Molecular Medicine. mRNA expression of genes of interest MACC1 and IER2 were measured using RT-qPCR using tumor samples of 60 patients with metastatic CRC. These samples were obtained from 60 patients at stages I, II, or III. Detailed information on patients and tumor tissue is provided in previous reports.[32, 54, 55]

4.2.9 Data mining of Expression Microarray data

The Gene Expression Omnibus (www.ncbi.nlm.nih.gov/geo) was used to search for publicly available expression data of CRC tumor microarrays. Expression data for target genes MACC1 and IER2 were obtained and normalized to expression data of Glyceralsdehyde 3-phosphate dehydrogenase (GAPDH). They were consecutively analyzed for direct or inverse correlation. GDS4718 [56] was accessed and analyzed.

4.2.10 Statistical analysis

Statistical analysis was performed using GraphPad Prism Version 6. Correlation analyses were using Pearson's r. Comparison of the control with multiple groups was carried out using a one-way analysis of variance (ANOVA). Comparisons between two groups was carried out using the unpaired t-test. Survival rates were calculated with the Kaplan–Meier estimator. The cut-offs to distinguish low and high expression levels were determined using the Receiver–operator-characteristics (ROC) analysis by taking the value with the highest Youden-Index. Statistical significance was set at $p < 0.05$ (*), $p < 0.01$ (**) and $p < 0.001$ (***).

5 RESULTS

5.1 Clinical evidence of MACC1 and IER2 overexpression and co-occurrence

Both MACC1 and IER2 mRNA levels in patient tumor samples were investigated and the cumulative survival against time in months was plotted in Kaplan-Meier plots. Figure 10 demonstrates that patients with higher IER2 expression lived significantly shorter than patients with low IER2 expression. Similarly, MACC1 expression values also showed a significant impact on patient survival. A high MACC1 expression was associated with shorter survival for these patients. To test for improved risk stratification in a combined analysis of IER2 and MACC1 expression, OS was evaluated for the subgroups low MACC1 and high IER2, high MACC1 and low IER2, both high MACC1 and IER2, and both low MACC1 and IER2, where a significantly shorter cumulative survival was found in patients with high expression of both MACC1 and IER2. Conversely, a low concentration of both markers was linked to the longest survival. High tumoral expression of IER2 mRNA was associated with a 10-year survival of approximately 50%, whereas patients with a low expression of IER2 showed a 10-year survival of approximately 80%. High tumoral expression of MACC1 resulted in a 10-year OS of circa 30% whereas patients with a low expression of MACC1 had a 10-year overall survival of close to 70%. Further scrutiny of the Kaplan-Meier curves (Fig. 10C) shows a 5-year OS survival for patients with both high IER2 and MACC1 mRNA expression levels of 50% and a 10-year OS of 30%. Conversely, when the expression of both genes was low, 5- and 10-year OS was over 90%.

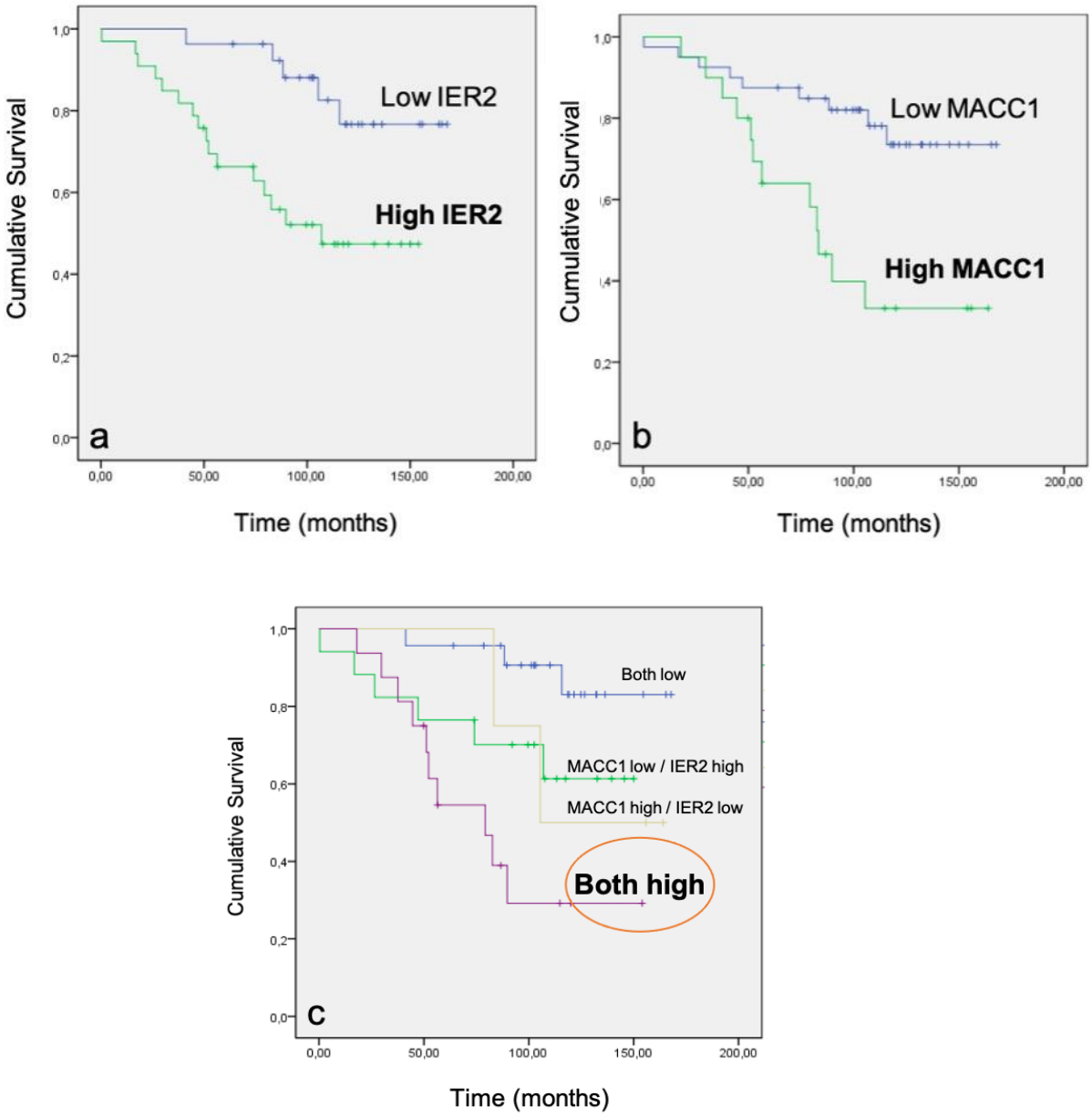

Figure 10

Kaplan-Meier plots depicting various MACC1 and IER2 mRNA expressions (high and low) against cumulative survival. Patients were divided by either high or low mRNA expression of IER2 and MACC1. a) Higher IER2 mRNA expression leads to worst cumulative survival. b) As expected, and previously reported, higher MACC1 mRNA expression translates into poorer cumulative survival. c) Patients who expressed high levels of both MACC1 and IER2 were also the patients with the worst outcome measured in cumulative survival over months. Plots were calculated by Marc Osterland of the Stein working group at the Max Delbrück Center for Molecular Medicine. Unpublished data.

5.2 Robust positive correlation of MACC1 and IER2 transcripts in *in silico* analysis

Our findings were confirmed by making use of the NCBI's Gene Expression Omnibus (GEO) database as described in the methodology. GDS4718[56] contains expression analysis from homogenized CRC tumors representing various disease stages with and without metastases from 44 patients. Expression values of MACC1 and IER2 were extracted from the dataset, along with the values for GAPDH, a stably expressed housekeeping gene. Normalized values were gathered in an XY table and plotted accordingly. Datapoints are shown in Figure 11. Making use of Pearson's r correlation analysis, the IER2/MACC1 axis showed a significant positive correlation (R^2=0.7544).

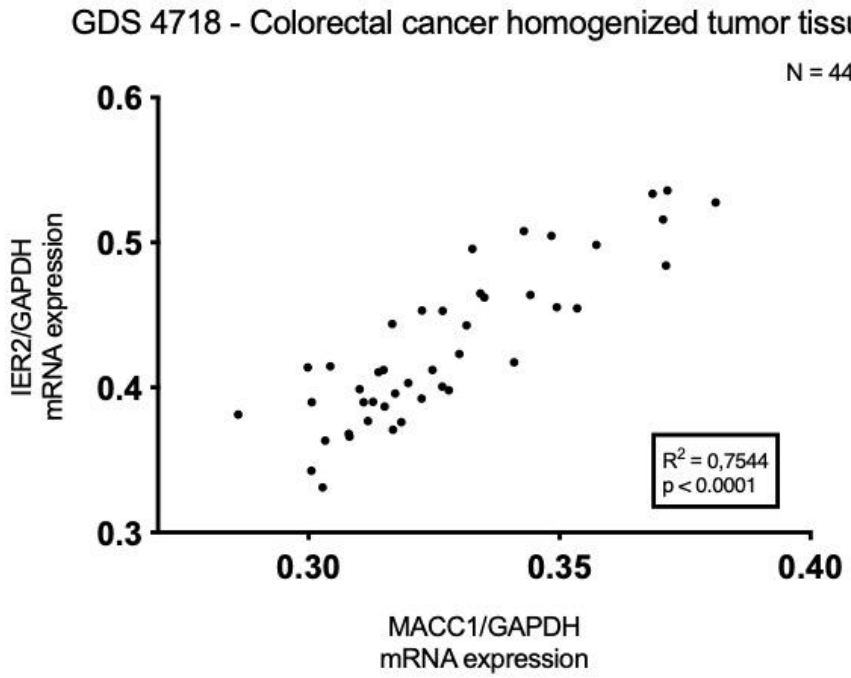

Figure 11

Correlation analysis using data from GEO DataSet number GDS4718[56] that positively correlates MACC1 and IER2 mRNA expression. Normalization against GAPDH and mapped in a XY plot. Significance was set at $p < 0.05$.

5.3 *In silico* prediction of IER2/MACC1 protein-protein interaction

Following a positive in silico correlation of our two genes of interest at the mRNA level, a further revision of curated databases for predictive protein interaction and interaction sites was carried out. To acquire an overview of possible protein interactors the String

Network[57] (www.string-db.org) database was consulted. When searching for "IER2 – homo sapiens", the following predicted functional partners are returned: EGR1, BTG2, JunB, FOS and GRB2 among others (ordered from highest to lowest assigned score: 0.850 – 0.636). These predicted interactions are meant to be specific and meaningful, and in consequence, are not necessarily meant to bind to each other but rather contribute to a shared function. Furthermore, these associations were predicted through text mining and co-expression analysis such as, but not limited to, anti-bait co-immunoprecipitation assays or tandem affinity purification assays. Therefore, direct experimental validation is still needed. A figurative representation of the IER2 and MACC1 networks according to the String Database are depicted below (Fig. 12).

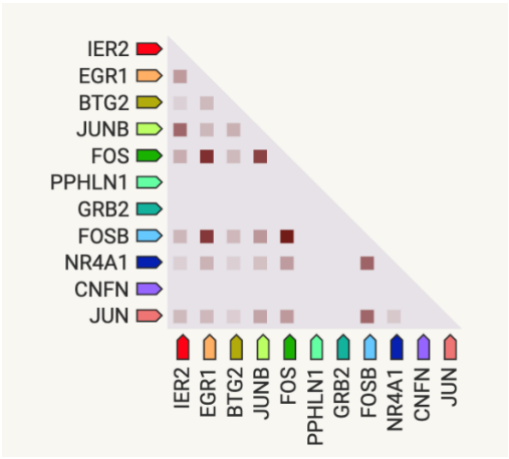

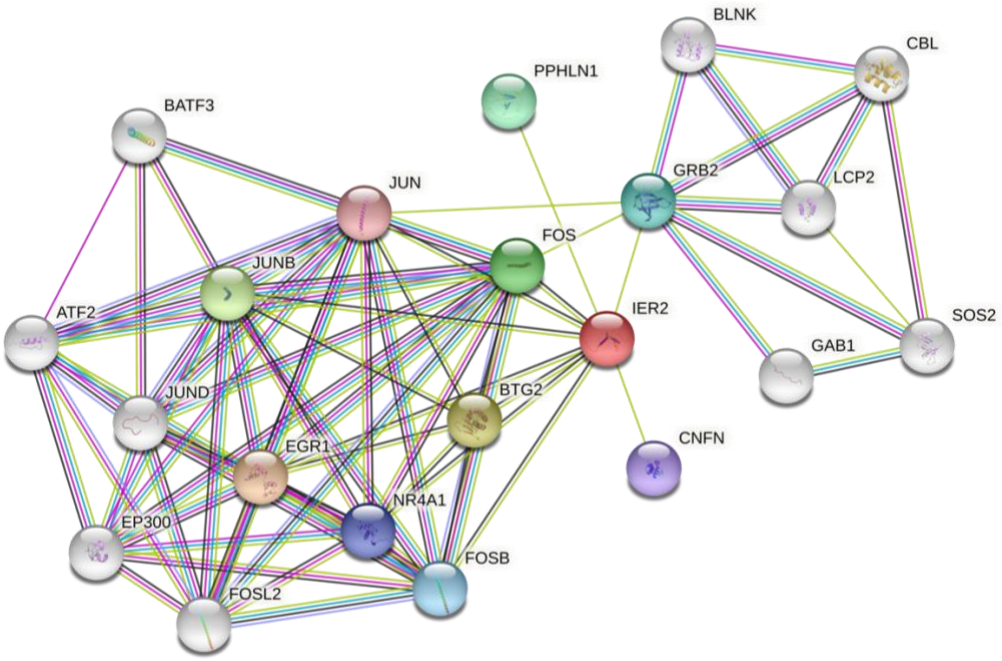

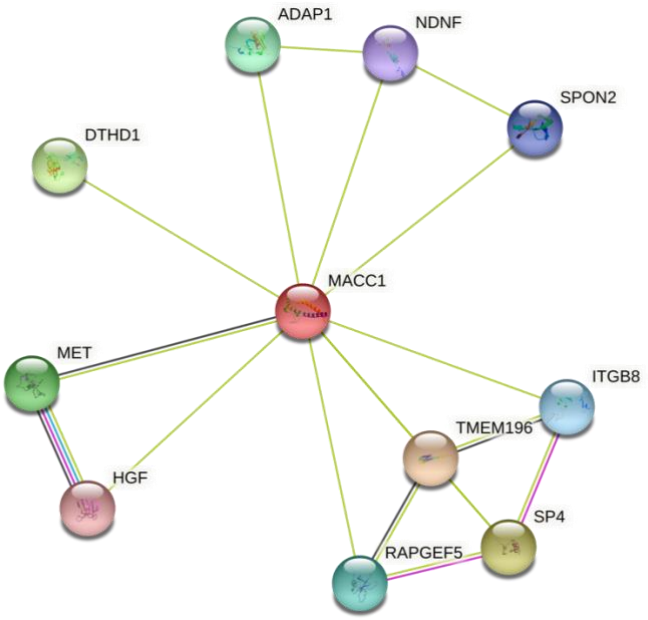

Figure 12

Representation of the IER2 and MACC1 protein-protein associations network. Predictions from the String Network[57] Database. Highest predictive scores for IER2 in text. Top (p. 48): IER2 heatmap. Coexpression scores based on RNA expression patterns, and on protein co-regulation provided by ProteomeHD (www.proteomehd.net/). Darker squares mean higher scores. Middle: IER2 String network. Bottom: MACC1 String network. Lines represent protein protein associations: light blue: know interactions from curated databases, pink: known interactions experimentally determined, green: predicted interactions based on gene neighborhood, red: predicted interactions based on gene fusions, royal blue-: predicted interactions based on gene co-ocurrence, light green: textmining, black: co-expression, lila: protein homology.

5.4 MACC1 and IER2 are co-expressed within cancer cells

To validate the previous findings *in vitro*, we used human colon adenocarcinoma derived SW480 cells which do not express endogenous MACC1. A stable MACC1 overexpressing cell line was developed in our laboratory. MACC1 cDNA transfection not only led to a strong increase in MACC1 ($p < 0.0286$), but also to a 20-fold upregulation of the IER2 mRNA expression in comparison to the empty vector (ev) control ($p < 0.0286$). This was confirmed on the protein level (Fig. 12). As a counterpart, SW620 cells, which are derived from a metastasis in the same subject whose primary tumor yielded the SW480 cell line,[32] have an endogenously high amount of MACC1. Stable transfection

of MACC1-specific small hairpin RNA (shRNA) strongly decreased MACC1 mRNA expression ($p < 0.0001$) as well as IER2 mRNA expression ($p < 0.0278$). Confirmation was also acquired at the protein level (Fig. 12).

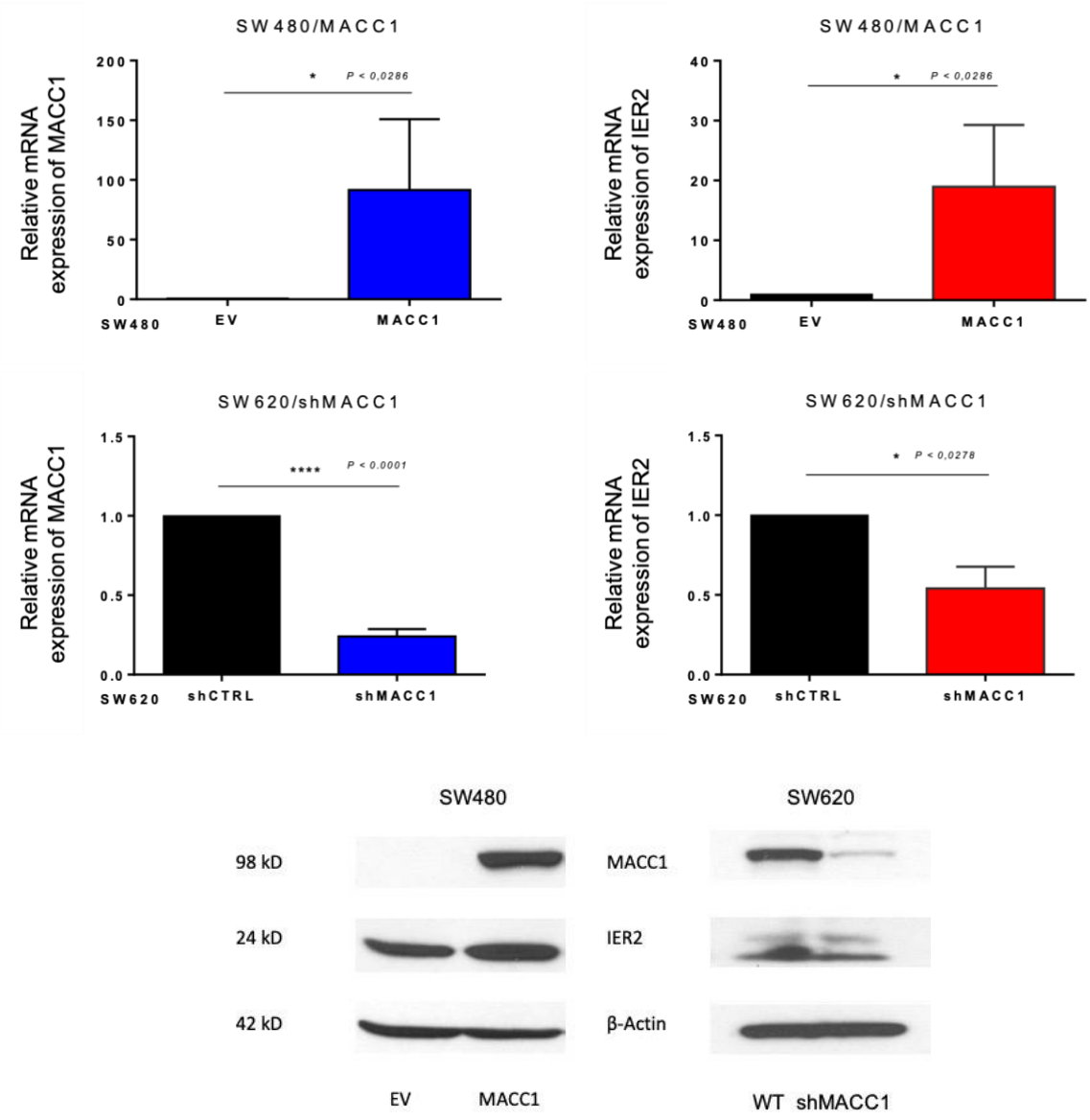

Figure 13

MACC1 and IER2 mRNA and protein expression in two CRC model cells. Top: Bar graphs showing mRNA expression of MACC1 and IER2 in SW480/MACC1 transfected cells and SW480 ev control cells (upper), as well as mRNA expression of MACC1 and IER2 in SW620/shMACC1 transfected cells and SW620/shCtrl control cells (lower). Significance was set at $p < 0.05$. Bottom: Western blot of SW480/ev and SW480/MACC1 cells (left), as well as SW620/shMACC1 and SW620/shCtrl cells (right). MACC1 and IER2 were blotted in both cell lines. β-Actin was used as a loading control.

A tetracycline-induced system was used to investigate a possible conjunction between MACC1 and IER2. A HCT116 cell line with a tetracycline-induced MACC1 promoter was used in this experiment. The tetracycline used in this system was Doxycycline. After exposing the cells to Doxycycline, the mRNA levels were measured using RT-qPCR at two time points (0 and 4 h) after exposure. These experiments were also carried out using the SW620 cell line, with a short hairpin MACC1 (shMACC1) tetracycline-induced construct. In this setting, a 2 h time point was also measured.

MACC1 overexpression was significantly evidenced 4 h after Doxycycline stimulation reaching a 2.65-fold increase in mRNA expression normalized to the housekeeping gene Ribosomal Protein L32 (RPL32). Concomitantly, IER2 followed with a 30% increase of expression in comparison to the untreated control. Additionally, as a counterpart, a MACC1 downregulation model was also used. Exposure to Doxycycline after 2 h significantly reduced the mRNA expression of MACC1 by 70% (again normalized to the housekeeping gene RPL32) in comparison to the control without drug exposure. Concomitantly, an IER2 mRNA expression reduction of about 30% was evidenced. This showed no significance. After 4 h of exposure, both MACC1 and IER2 mRNA expressions were significantly reduced by 99% and 76%, respectively (Fig. 13).

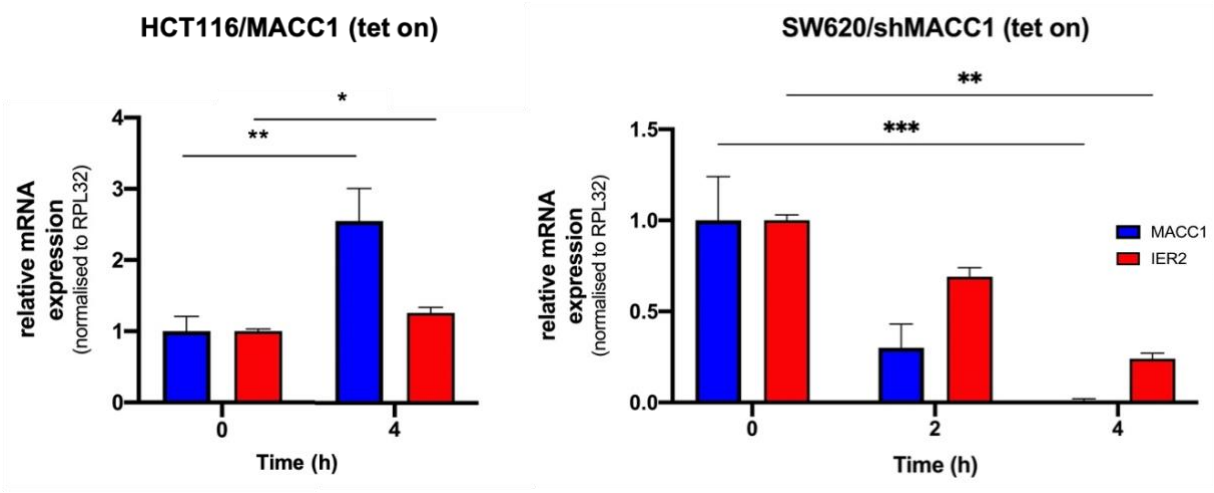

Figure 14

Bar graph showing mRNA expression of MACC1 and IER2 after treatment with Doxycycline in a tetracycline-induced HCT116/MACC1 system (left) and a tetracycline-induced SW620/shMACC1 system (right). Relative mRNA expressions have been normalized to the housekeeping gene RPL32. Time is expressed in hours after exposure to the drug. Significance was set at $p < 0.05$.

Following the *in silico* prediction of a possible SH3-mediated MACC1-IER2 interaction, a Co-IP assay using SW480/MACC1 transfected cells was carried out in order to prove direct protein-protein interaction. The blot shown in Fig. 14 demonstrates an IER2 protein pulldown in MACC1 overexpressed cells. The input column shows MACC1 and IER2 protein expression in the sample. Anti-β-Tubulin was used as a negative control. Under the column denominated MACC1, a band at the 24 kDa mark demonstrates IER2 protein bound to the MACC1 protein acting as the antigen in the assay, indicating an encouraging interaction between MACC1 and IER2 proteins.

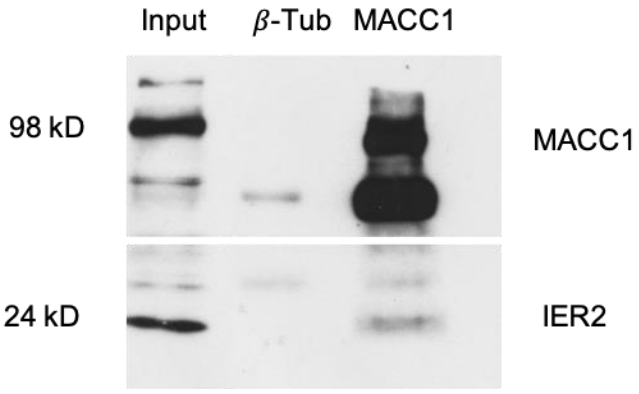

Figure 15

Co-immunoprecipitation blot demonstrating a successful IER2 pulldown and direct evidence for a MACC1/IER2 protein interaction. Anti-β-Tubulin was used a negative control. IER2 molecular weight: 24 kDa, MACC1: 98 kDa.

5.5 Functional synergism of MACC1 and IER2 *in vitro*

5.5.1 Colony formation

For the following experiment, HCT116 modified cells were used. These were transfected with IER2, yielding an overexpressing IER2 HCT116 (HCT116/IER2) cell line. These cells were kindly provided by Dr. Jonathan Sleeman's group and engineered by Dr. Lenka Kyjakova. Various ev and IER2 overexpressing cells were sent to our laboratory. After checking IER2 mRNA overexpression in the cells, the highest IER2 yielding cell line was used for the subsequent experiments. As mentioned above, the plates were photographed and later analyzed. Figure 15 demonstrates a higher colony count in cells overexpressing IER2. The colony count number was significantly higher in cells overexpressing IER2 in comparison to the empty vector control cells.

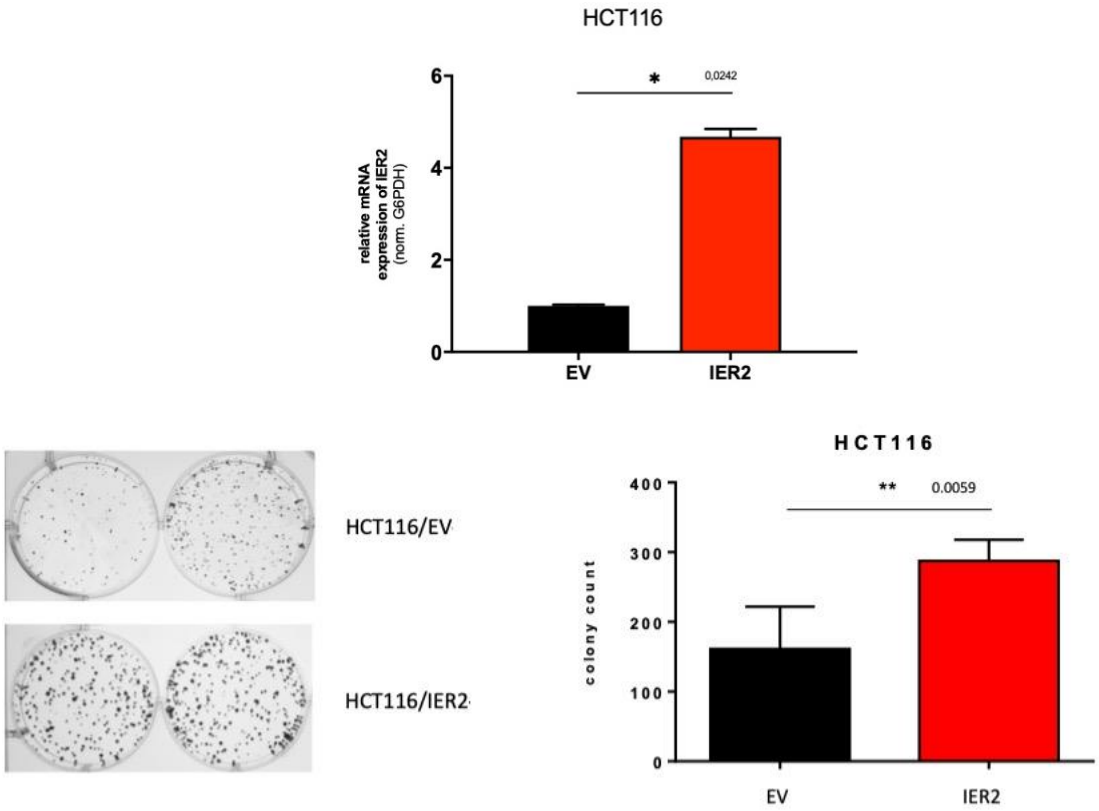

Figure 16

Colony formation in overexpressed IER2 CRC cell line. Top: Bar graph showing successful mRNA overexpression of IER2 in HCT116 cells transfected with IER2 ($p < 0.0242$). mRNA expression was normalized to the housekeeping gene G6PDH (above). Collage of six-well plate photographs to compare colony formation between IER2 overexpressing HCT116 (HCT116/IER2) cells and control (HCT116/ev) cells (left). Bar graph translating picture collage, where a significantly higher number of colonies were formed by IER2 overexpressing cells ($p < 0.0059$) (right). Significance was set at $p < 0.05$.

5.5.2 Proliferation Assay

Further functional testing was carried out using the modified IER2 overexpressing HCT116 cells. A proliferation assay was carried out to elucidate IER2's involvement in cell division. This assay uses snapshots at previously set time points to measure relative confluence, which then extrapolates to cell proliferation. Figure 16 depicts a curvilinear graph of a HCT116/IER2 cell line against an empty vector control. After 96 h in the incubator, the IER2 overexpressing cells proliferated more in comparison to the HCT116/ev cells. However, this effect showed no statistical significance.

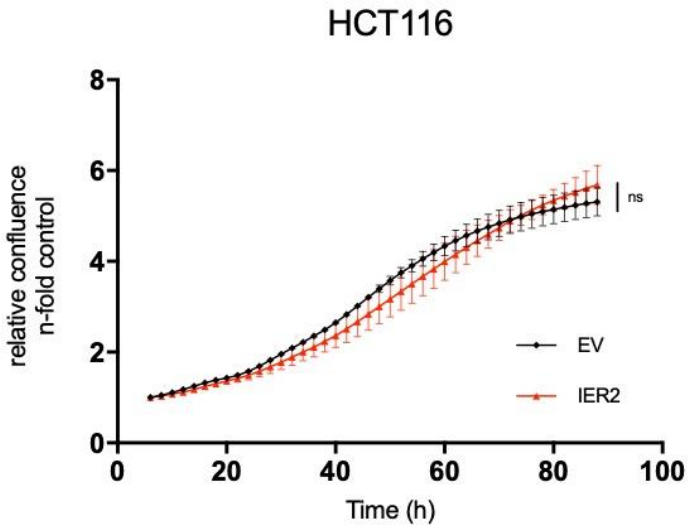

Figure 17

Curvilinear graph depicting relative confluence against time in hours of a HCT116/ev cell line and a HCT116/IER2 cell line. No significance was achieved in this experimental setting. Results represent means + SEM of three independent experiments. Significant results were determined by two-way ANOVA and Sidak's multiple comparison test. Significance was set at $p < 0.05$.

Furthermore, the same assay was carried out using our IER2 knockout (KO) cell line model. The following figure depicts a curvilinear graph of a SW620/Cas-9 empty vector control cell against a SW620/KO-IER2 cell line. The calculations were made after cells spent 96 h in the incubator. IER2-depleted cells proliferated significantly less than the Cas9-EV control cells. Statistically significant changes can be observed after the 56 h time point. After 96 h, proliferation of cells where IER2 was knocked out was about 35% less in comparison to the control cells.

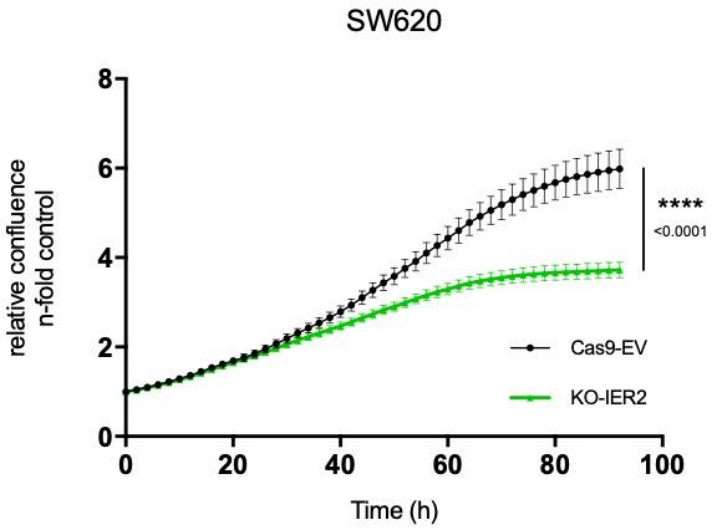

Figure 18

Curvilinear graph depicting relative confluence against time in hours of SW620/Cas9-ev in comparison to SW620/KO-IER2. Proliferation was significantly decreased in absence of IER2. Time is indicated in hours. Results represent means + SEM of three independent experiments. Significant results were determined by two-way ANOVA and Sidak's multiple comparison test. Significance was set at $p<0.05$.

6 DISCUSSION

For these CRC-associated markers, the best efforts have been put into answering questions regarding their molecular interplay, the presence or absence of a functional MACC1/IER2 relationship, and finally, reaching a conclusion as to a synergistic collaboration between them. Ultimately, this has contributed to knowledge of the IER2-induced mechanisms that translate into such poor prognosis for CRC patients.

6.1 Concomitant overexpression of MACC1 and IER2 translates into worse patient survival

With an ever-growing body of knowledge about the molecular mechanisms behind tumor initiation, local progression and transformation, and lastly, metastasis, there is a wealth of novel and pathway-specific markers, yet few have been approved as cancer markers for detection or risk stratification, let alone treatment selection. Nevertheless, gene products with distinct functional effects in the process of carcinogenesis could particularly qualify as prognostic and predictive biomarkers.[25, 58, 59] MACC1's capability to weigh in on therapeutic decision-making as well as to clarify a patient's prognosis is exactly what makes it a valuable biomarker. It is both predictive, as it may soon be used to veer therapeutic decisions, and it is prognostic as previously mentioned. To better understand the biomarker's impact on patient survival, Kaplan-Meier survival graphs have been used standardly. They illustrate and thus facilitate our understanding and assessment of patient treatment options. Cumulative survival for patients with higher expression of IER2 and MACC1 genes was significantly worse. This was true when they were analyzed separately as well as when they were analyzed in patients with both highly concomitant IER2 and MACC1 expression. Analysis carried out by a member of our group reveals that the worst survival expectation belongs to patients with both high IER2 and MACC1 mRNA expression in their tumors, with approximately 50% of patients not living past 4 years. Further analysis indicates that about 50% of patients with higher IER2 mRNA expression in their tumor samples had passed away after 10 years, whereas approximately 80% were still alive if IER2 mRNA expression was categorized as low. Moving on to MACC1, 50% had passed away earlier, after around 80 months. On the

other hand, after the same amount of time, roughly 85% of patients, whose tumors were categorized under “low MACC1” expression, were still alive.

It is understandable how MACC1 would elicit such an impoverished survival rate, given the fact that it is an established biomarker for the prognosis of distant metastasis formation.[32] MACC1 mRNA expression was higher in tumors that had not yet metastasized but did later (metachronous) in comparison to those that did not (Fig. 18). When MACC1 alone is overexpressed, patients succumb earlier and also more frequently to the disease.

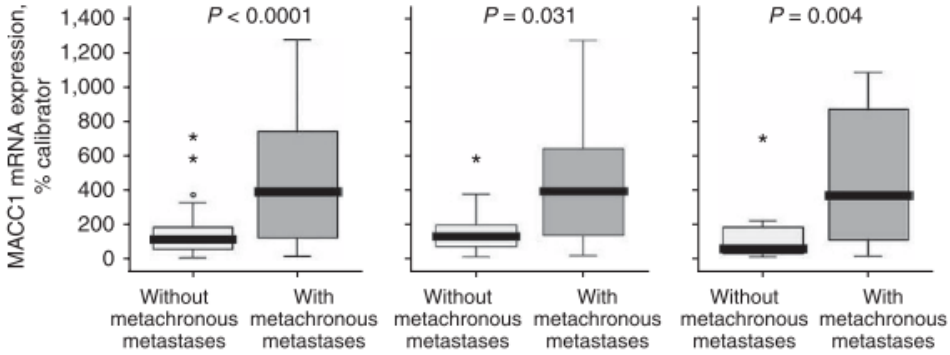

Figure 19

Bar graphs showing MACC1 mRNA expression in primary colorectal tumors. UICC stages 1-3 (left), UICC stages 1 and 2 (middle), and UICC stage 3 (right) as determined by RT-qPCR. Stein et al.[32]

For IER2 this is a new finding. Although our clinical findings support IER2 playing a dramatic role in overall patient survival, it is unlikely that it achieves this effect on its own. The fact remains that there is not enough information published about the protein or the gene to accurately explain this phenomenon. When it was initially discovered, IER2 was linked to cellular apoptosis and necrosis – specifically in neuronal cells. Its discovery was primarily in the involvement of cell-death mechanisms in the brain and cells outside the central nervous system.[60, 61] After some years in the background, IER2 came to light again when it was found to be upregulated in many human tumor types and that it correlates with poor patient survival. Neeb *et al.* also showed how IER2 overexpression correlated with poor metastasis-free and overall survival of patients with CRC (see reference Fig. 5, panels b and c).[48]

An *in silico* analysis making use of the GEO Database and its “DataSet” records provided further insight into a possible MACC1/IER2 axis. GDS4718 provides “insight into predictive biomarkers of metastasis and treatment targets in CRC”[56] as it contains expression values taken from previously homogenized CRC tumors that represented diverse disease stages both with and without metastases. A strong positive correlation was found between MACC1 mRNA expression and IER2 mRNA expression in this dataset. The positive correlation between MACC1, an established prognostic and predictive biomarker in CRC, and IER2, a novel contestant in this field, drove this investigation toward finding the molecular interplay that these two genes could have. Upon reviewing the literature and our findings, IER2 may not yet be an established predictive biomarker for cancer, but it may well be a prognostic biomarker.

6.2 MACC1 and IER2’s co-expression and simultaneous downregulation

Probing into CRC cell lines to acquire a first snapshot of a possible interaction between both genes of interest, the proven SW480 and SW620 CRC cell lines were analyzed. In stably MACC1-transfected cells, a concomitant IER2 mRNA overexpression was observed. This was translated as well at the protein level. Western blots showed a higher signal at IER2’s 24 kDa band when in presence of MACC1. Furthermore, taking advantage of the SW620/shMACC1 cell line, IER2 mRNA expression was also found to be reduced under suppressed MACC1 mRNA expression. Translation at the protein level was also evidenced, i.e., in a less visible IER2 band in absence of MACC1.

Taking advantage of the tetracycline induced - or tet-on - model previously developed in our laboratory, MACC1 modulation was achieved after Doxycycline treatment. Both overexpression and downregulation were successfully achieved with a HCT116/MACC1 cell line model and a SW620/shMACC1 cell line model respectively.

IER2, as an immediate early response gene, reacted in a shorter time period in comparison to MACC1. Nevertheless, MACC1 held its overexpression over time, whereas IER2 expression was decreased at the 4 h time point. This corroborates the general knowledge that IEGs peak out relatively fast and after 2 hours are at roughly normal levels. By observing the short hairpin model, what stands out is the time needed

to impact IER2 expression. As a readily available molecule in the cytoplasm, it would be expected that downregulation would take time as the already present IER2 must first be depleted. Nevertheless, after 4 hours, IER2 diminished mRNA expression after Doxycycline mediated MACC1 downregulation was, at 24% of the original amount, significant.

Could this mean that MACC1 drives IER2 expression? It is difficult to arrive at a conclusion just from these experiments, and especially when taking into consideration protein expression levels in this setting, which have shown some confounding results. To date, no known mechanism directly explains MACC1's involvement in IER2's expression. As IER2's induction is mainly triggered by sera, growth factors, TPA and membrane depolarization,[62] MACC1's role at this higher level would be unlikely. The serum response element (SRE) is the main regulatory element located in the IER2 promoter region, although transcription factors of the Ets family also play a role in IER2 induction.[62]

Deepening of the understanding of this clinically relevant synergy requires revisiting possible pathway overlaps that MACC1 and IER2 may share. In a thorough MACC1 review published in 2019, Radhakrishnan *et al.* [25] shed light on the last decade in MACC1 research. Among a substantial number of MACC1-driven processes, the sustaining of proliferative signaling and activating of metastasis through the PI3K/Akt pathway as well as the evading of growth suppressors are of particular interest in the IER2 context. MACC1 plays an important role in these processes by being atop of diverse pathway axes as it is a c-MET transcription factor. IER2 does not seem to play a role so far upstream, but may well collaborate by modulating inhibitory phosphatases, e.g., PP2A. More interestingly, remaining in the IER2 context, MACC1 was shown to induce G_1-S cell cycle progression by inhibiting Phosphatase and tensin homolog (PTEN), a PI3K/Akt pathway inhibitor, whereas IER2 contributes to the same end through a cell cycle inductor, namely CDC25A. This will be further discussed in a coming subchapter.

6.3 IER2/MACC1 protein-protein interaction

Following transcriptomics, further experimentation was carried out to prove a possible protein-protein interaction between MACC1 and IER2. As mentioned before, the String

Consortium database was consulted. This web-based tool is used, among other scenarios, to show network connectivity. It is of importance to clarify the use of scores. According to the information provided by the String Consoritum, scores are are not to be interpreted as the “strength or the specificity of the interaction” but rather they are indicators of confidence. The network judges “an interaction to be true, gven the available evidence.” Using a scale from 0 to 1, with 1 being the highest possible confidence. The highest scored interaction for IER2 is with transcriptional factor JUNB (0.850). Further research into this association makes it clear that there is an experimental gap to be addressed. Although there is some literature envolving IER2 and JUNB, it is only to denote the known fact, that both are immediate response genes that will be present in acute phases of cellular stimulation.

To further investigate to what extent, and how exactly a possible IER2 and MACC1 protein interaction could take place, the Eukaryotic Linear Motif (ELM) resource for functional sites in proteins [63] was consulted. This web-based resource predicts protein interaction sites. A search for IER2 (or Q9BTL4 – UniProt identifier) produced a total of 53 predicted ELMs, 40 of which remained after being filtered for species, structural score, and cellular location. After careful analysis, one predicted site is of interest: “LIG_SH3_3”. As its name references, this site is a Src homology 3 (SH3) ligand. These well-known domains are small protein modules that bind to proline-rich peptides. Four instances were found to be highly probable SH3 ligand domains: EPEVSLP, AALPSDP, NCSPAAP, and AAPPTAP. In the seminal work carried out by Stein *et al.* [32], a SH3 domain in the MACC1 protein was identified. In this respect, it would be possible to speculate that, seeing as IER2 has four binding regions for SH3, a probable SH3-mediated protein interaction may occur between our two proteins of interest. This in silico result led us to carry out a Co-IP assay where IER2 was to be pulled down in cells where a high protein expression of MACC1 is known to be expressed. As mentioned before, an overexpressing SW480/MACC1 transfected cell line was used. IER2 was successfully blotted after successful pulldown, which suggests a protein interaction as most likely through the aforementioned association.

6.4 IER2 overexpression enhances clonogenicity

Continuing in the pursuit of finding a possible MACC1/IER2 interaction at the molecular and protein levels, work continued in the search for understanding how IER2 could contribute to metastasis formation. Therefore, functional assays were carried out to understand which cell mechanisms could be used to achieve better metastasis formation capabilities. A colony formation assay was carried out initially. The objective was to better understand IER2's possible influence over tangible cellular activity. This assay focuses on the modified cells' capacity to form colonies. Stably IER2-transfected HCT116 CRC cells were used in this experiment. These were engineered in the laboratory of Prof. Jonathan Sleeman by Dr. Lenka Kyjacova from the University of Heidelberg in Germany. The statistically significant results showed a higher colony formation capacity from the IER2 transfected cells in this colorectal cancer model.

IER2 is known to be a regulator of the cell cycle G_1-S transition. A novel Bayesian model, used to generate predictions regarding components needed for the cell cycle, efficiently predicted known cell cycle components such as CDC25A, but also IER2, to be involved in the G_1-S transition.[64] In accordance with this finding, IER2 has been found to interact with CDC25A through the 14-3-3 protein.[65] This regulation is mediated at the T507 residue, which appears to be located within a cyclin B1/cyclin-dependent kinase 1 (CDK1) site in the C terminus of CDC25A.[65] By dephosphorylating T507, IER2 inhibits the interaction of CDC25A with 14-3-3, one of its regulatory proteins, therefore activating CDC25A. CDC25A, as a critical part for cell proliferation, is strongly regulated. Running amok, CDC25A will rapidly affect the cell cycle through dephosphorylation and activation of CDKs required at the G_1-S transition and G_2-M boundary.[50] Therefore, a dysregulated cell cycle through CDC25A dysfunction could contribute to the explanation of why IER2 overexpressing cells have the ability to form more colonies.

6.5 Absence of IER2 hinders cellular proliferation

Following the evidence that IER2 overexpressing cells form more colonies, the next step was to investigate further into the question of the proliferation of these colonies. To

this end, a proliferation assay was carried out using a SW620 CRC cell line model. The IER2 gene was knocked out using CRISPR/Cas9. This assay focuses on measuring deltas in relative confluence in low-seeded plates by taking images over 4 days. Wherever the SW620 IER2 knocked out cells were plated, the relative confluence area was significantly lower than in their counterparts. In this respect, IER2 would be needed for cellular proliferation.

PP2A is a major ubiquitously expressed serine/threonine phosphatase. Its functions range from taking part in major cell signaling pathways that regulate cell cycles and metabolism as well as cell migration and cell survival.[66–68] PP2A is a complex of 3 specific and individual subunit proteins that function as a heterotrimeric holoenzyme. The core dimer consists of a scaffolding subunit (A) and a catalytic subunit (C). When the core dimer interacts with the B regulatory subunit, the enzyme reaches its full activity, specific subcellular location and substrate specification.[66, 68, 69] PP2A's role in the regulation of growth factor signaling is particularly interesting, and even more so, its involvement in cell proliferation.[66] Multiple families and isoforms of both the A and B subunits further increase the diversity of PP2A. The PP2A holoenzyme containing PP2A-B55α has been identified as a regulator of Protein Kinase B (Akt) phosphorylation at T308, acting to negatively regulate Akt-mediated cell proliferation and survival.[70] Another example is PP2A's inhibition by dissociation of PP2A from the adaptor protein Shc, leading to increased and sustained Shc phosphorylation, as well as consequent activation of the MAP kinase pathway to promote cell proliferation.[66, 68] When IER2 was pulled down in a HeLa cell model study aimed at studying IER2 interaction with PP2A's subunits, evidence was provided to show that IER2 binds through its N-terminal to all four B55 Units (including B55α).[47] In this sense, IER2 - along with other IER proteins - regulates the phosphorylation status of PP2A-B55 targets. Conclusively, IER2 could arguably be a PP2A activator and an enhancer of its phosphatase activity.

Were this the case, one would assume that PP2A activation, and its consequent dephosphorylation of Akt, and with it, the deregulation of the known downstream effects of the mTOR pathway, would lead to diminished protein synthesis, apoptosis mediated by FOXO proteins and overall catabolism. This was, however, not observed in our findings when IER2 was knocked out. Absence of IER2 led to a significant reduction of

the cells' capacity to proliferate, an unexpected finding in an Akt upregulated scenario. Nevertheless, if we go back to Ueda *et al.'s* [47] recent research on the IER family proteins, we find a remarkable conclusion regarding the downstream mTOR effector S6 kinase (S6k). Interestingly, they found that IER2 induced hyperphosphorylation of S6k. Upon expression of IER2, phosphorylation levels at the T421 and S424 residues were not reduced. To their knowledge, this hyperphosphorylation must be mediated upstream given that there is no site for IER2 in the S6k complex. Where this regulation may take place must still be experimentally proven. In 2010, Goh *et al.* [71] studied the mTOR/S6k complex's role in heterogeneous ribonucleoprotein (hnRNP) activation. These are chromatin-associated RNA-binding proteins in charge of RNA splicing, internal ribosome entry site translation, RNA polymerase II regulation, and telomeric regulation.[71, 72] In their findings they describe a functional mTOR-S6k2-hnRNP F complex capable of regulating cellular proliferation by mechanisms that are still to be elucidated. Were IER2 to contribute to a transient cell proliferation activation signal through hyperphosphorylation of S6k, the proven pathway found by Goh and colleagues may well be the explanation behind the mechanism.

To examine the consequences of augmented IER2 expression, the same assay was carried out with the IER2 overexpressing HCT116 CRC cell line. In this model, it was observed that IER2 overexpression did not evoke enhanced cellular proliferation capabilities. This may suggest that IER2 has a role to play in cellular proliferation, but that above a certain threshold of IER2 expression, no further proliferation will be induced.

6.6 MACC1 and IER2 – a synergistic collaboration?

An important question that this thesis aimed to tackle concerned a MACC1 and IER2 dependency. This question remains open, given the fact that IER2 is a scarcely investigated molecule, and its interactions are practically unknown. The suggestions derived from the work presented here point toward a functional link, i.e., independent mechanisms that work in synergism to confer cancer cells enhanced metastatic capabilities.

MACC1 sits atop of crucial metastasis-inducing, proliferation-enabling, angiogenesis-contributing, and c-MET-driven axes. In short, c-MET upregulation by MACC1 is vital in

activating downstream signaling mechanisms, such as PI3K/AKT/β-catenin, STAT1/3, MEK/ERK, and TWIST/VEGF, resulting in cellular processes involved in oncogenic transformation, tumor progression and lastly, metastasis formation.[25, 32, 73–75] Pertaining to our subject, MACC1 promotes a strong HGF/c-MET proliferation signaling by activating downstream GAB-SHP2-ERK/MAP and PI3K/AKT effector axes, and as MACC1 itself is regulated by ERK, a positive feedback loop emerges and represents a self-sustaining proliferation mechanism.

Looking further into the *in silico* protein interaction predictions using the ELM web-based resource, several other interesting motifs are found in the small IER2 protein. Binding motifs for kinases that mediate interaction towards ERK1/2 and p38 (DOC_MAPK_MEF2A_6), Casein kinase 1 (CK1) and CK2 (formerly casein kinase 2) phosphorylation sites (LIG_CK1_1 / _2), PKA and PKB phosphorylation sites (MOD_PKA_1 / _2) and binding motifs for proteins with SH2 domains were among many other interesting predictions returned. Both MACC1 and IER2 share similar motifs, i.e., SH2 and SH3 domain binding motifs, MAP kinase binding regions and CK phosphorylation recognition sites. A broader speculation is that MACC1 and IER2 form yet-to-be proven protein complexes by attaching to the same kinases and/or other substrates, thus working in conjunction. Were this the case, this synergistic collaboration would directly and/or indirectly be linked to important cellular signaling pathways such as the PI3K/Akt, β-catenin/Wnt, and JAK2/STAT3 pathways among others. In this regard, Kyjacova *et al.* [53] showed that the Akt pathway is activated by IER2 and involved in context-dependent cytokinesis failure. This results in aneuploidy in cancer cells, and drives tumorigenesis through genomic instability.[53, 76]

Breakthrough data published recently has found a direct relation between IER2 expression, its nuclear localization, and senescence. IER2-induced senescence and OPN production is p53 dependent.[53] An IER2-mediated SASP could plausibly stimulate the growth and aggressiveness of non-senescent tumor cells in the microenvironment. Specifically, secreted OPN would promote tumor growth and metastasis, for example through the activation of receptors CD44 and integrins. These would consequently activate a sustained survival-, proliferation-, angiogenesis- and invasion-promoting signal.[53, 77]

6.7 Outlook

As has been well established through our work, IER2 offers a promising field of study to further unravel cellular mechanisms and protein complexes involved in the cellular proliferation, metastasis formation, and ultimately the worst clinical outcomes for our patients.

Further studies should be carried out to better understand IER2's role in hindering the capacity of cells to proliferate whilst promoting colony formation. This work achieved an IER2-KO model which could be further used for functional assays in the absence of IER2. Furthermore, using a SH3 deleted MACC1 mutant could be useful to corroborate the predicted association with IER2 via SH3 interaction.

Additionally, more light could be shed onto IER2´s role in enhancing PP2A´s phosphatase activity, as it is most likely, together with MACC1's interactions, to be its most important currently known effector. Moreover, functional assays with explicit IER2 and MACC1 direct manipulation are needed. Specifically, migration assays with MACC1 and IER2 overexpression, downregulation, and the combination of both, to advance our knowledge regarding MACC1/IER2 synergy. Lastly, IER2 and its new-found role in senescence must be further elucidated, as IER2-induced senescent cells may well be responsible, among other things, for cancer progression by direct cell cycle interference and chemoresistance, possibly through autophagy or by suppressing apoptosis.

The fact that IER2's presence exerts a significantly worse outcome for patients remains at the center of the reason why we must continue to pursue the understanding of its mechanisms of action.

7 BIBLIOGRAPHY

1. Sung H, Ferlay J, Siegel RL, Laversanne M, Soerjomataram I, Jemal A, Bray F (2021) Global Cancer Statistics 2020: GLOBOCAN Estimates of Incidence and Mortality Worldwide for 36 Cancers in 185 Countries. CA Cancer J Clin 71:209–249. https://doi.org/10.3322/caac.21660
2. Feig B, Ching CD, University of Texas M.D. Anderson Cancer Center (2019) The MD Anderson surgical oncology handbook, Sixth edit. Wolters Kluwer
3. Bray F, Ferlay J, Soerjomataram I, Siegel RL, Torre LA, Jemal A (2018) Global cancer statistics 2018: GLOBOCAN estimates of incidence and mortality worldwide for 36 cancers in 185 countries. CA Cancer J Clin 68:394–424. https://doi.org/10.3322/caac.21492
4. Arnold M, Sierra MS, Laversanne M, Soerjomataram I, Jemal A, Bray F (2017) Global patterns and trends in colorectal cancer incidence and mortality. Gut 66:683–691. https://doi.org/10.1136/gutjnl-2015-310912
5. Hölzel D, Schubert-Fritschle G, Schmidt M, Eckel R, Engel J (2016) Klinisch-epidemiologische Krebsregistrierung in Deutschland. Pathologe 37:371–387. https://doi.org/10.1007/s00292-016-0188-2
6. Song M, Chan AT, Sun J (2020) Influence of the Gut Microbiome, Diet, and Environment on Risk of Colorectal Cancer. Gastroenterology 158:322–340. https://doi.org/10.1053/j.gastro.2019.06.048
7. Makki K, Deehan EC, Walter J, Bäckhed F (2018) The Impact of Dietary Fiber on Gut Microbiota in Host Health and Disease. Cell Host Microbe 23:705–715. https://doi.org/10.1016/j.chom.2018.05.012
8. So D, Whelan K, Rossi M, Morrison M, Holtmann G, Kelly JT, Shanahan ER, Staudacher HM, Campbell KL (2018) Dietary fiber intervention on gut microbiota composition in healthy adults: a systematic review and meta-analysis. Am J Clin Nutr 107:965–983. https://doi.org/10.1093/ajcn/nqy041
9. Renehan AG, Zwahlen M, Egger M (2015) Adiposity and cancer risk: new mechanistic insights from epidemiology. Nat Rev Cancer 15:484–498. https://doi.org/10.1038/nrc3967
10. Shabanzadeh DM, Sørensen LT, Jørgensen T (2017) Association Between Screen-Detected Gallstone Disease and Cancer in a Cohort Study. Gastroenterology 152:1965-1974.e1. https://doi.org/10.1053/j.gastro.2017.02.013
11. Bernstein H, Bernstein C, Payne CM, Dvorak K (2009) Bile acids as endogenous etiologic agents in gastrointestinal cancer. World J Gastroenterol 15:3329. https://doi.org/10.3748/wjg.15.3329
12. Oldenhuis CNAM, Oosting SF, Gietema JA, de Vries EGE (2008) Prognostic versus predictive value of biomarkers in oncology. Eur J Cancer 44:946–953. https://doi.org/10.1016/j.ejca.2008.03.006
13. Guinney J, Dienstmann R, Wang X, De Reyniès A, Schlicker A, Soneson C, Marisa L, Roepman P, Nyamundanda G, Angelino P, Bot BM, Morris JS, Simon IM, Gerster S, Fessler E, De Sousa .E Melo F, Missiaglia E, Ramay H, Barras D, Homicsko K, Maru D, Manyam GC, Broom B, Boige V, Perez-Villamil B, Laderas T, Salazar R, Gray JW, Hanahan D, Tabernero J, Bernards R, Friend SH, Laurent-Puig P, Medema JP, Sadanandam A, Wessels L, Delorenzi M, Kopetz S, Vermeulen L, Tejpar S (2015) The consensus molecular subtypes of colorectal cancer. Nat Med 21:1350–1356. https://doi.org/10.1038/nm.3967
14. Pritchard CC, Grady WM (2011) Colorectal cancer molecular biology moves into clinical practice. Gut 60:116–129. https://doi.org/10.1136/gut.2009.206250

15. Fearon ER, Vogelstein B (1990) A genetic model for colorectal tumorigenesis. Cell 61:759–767. https://doi.org/10.1016/0092-8674(90)90186-I

16. Nguyen H, Duong H (2018) The molecular characteristics of colorectal cancer: Implications for diagnosis and therapy (Review). Oncol Lett. https://doi.org/10.3892/ol.2018.8679

17. Lengauer C, Kinzler KW, Vogelstein B (1998) Genetic instabilities in human cancers. Nature 396:643–649. https://doi.org/10.1038/25292

18. Markowitz SD, Bertagnolli MM (2009) Molecular Basis of Colorectal Cancer. N Engl J Med 361:2449–2460. https://doi.org/10.1056/nejmra0804588

19. Kinzler K, Vogelstein B (2002) The genetic basis of human cancer, 2nd ed. McGraw-Hill, New York

20. Issa J-P (2004) CpG island methylator phenotype in cancer. Nat Rev Cancer 4:988–993. https://doi.org/10.1038/nrc1507

21. Herman JG, Baylin SB (2003) Gene silencing in cancer in association with promoter hypermethylation. N Engl J Med 349:2042–54. https://doi.org/10.1056/NEJMra023075

22. Illingworth RS, Gruenewald-Schneider U, Webb S, Kerr ARW, James KD, Turner DJ, Smith C, Harrison DJ, Andrews R, Bird AP (2010) Orphan CpG Islands Identify Numerous Conserved Promoters in the Mammalian Genome. PLoS Genet 6:e1001134. https://doi.org/10.1371/journal.pgen.1001134

23. Boland CR, Goel A (2010) Microsatellite Instability in Colorectal Cancer. Gastroenterology 138:2073-2087.e3. https://doi.org/10.1053/j.gastro.2009.12.064

24. Weisenberger DJ, Siegmund KD, Campan M, Young J, Long TI, Faasse MA, Kang GH, Widschwendter M, Weener D, Buchanan D, Koh H, Simms L, Barker M, Leggett B, Levine J, Kim M, French AJ, Thibodeau SN, Jass J, Haile R, Laird PW (2006) CpG island methylator phenotype underlies sporadic microsatellite instability and is tightly associated with BRAF mutation in colorectal cancer. Nat Genet 38:787–793. https://doi.org/10.1038/ng1834

25. Radhakrishnan H, Walther W, Zincke F, Kobelt D, Imbastari F, Erdem M, Kortüm B, Dahlmann M, Stein U (2018) MACC1—the first decade of a key metastasis molecule from gene discovery to clinical translation. Cancer Metastasis Rev. 37:805–820 https://doi.org/ 10.1007/s10555-018-9771-8

26. Stein U (2013) MACC1-a novel target for solid cancers. Expert Opin. Ther. Targets 17:1039–1052. https://doi.org/10.1517/14728222.2013.815727

27. Wu Z, Chen L, Zhou R, Bin J, Liao Y, Liao W (2016) Metastasis-associated in colon cancer-1 in gastric cancer: beyond metastasis. 22:6629–6637. https://doi.org/10.3748/wjg.v22.i29.6629

28. Shimokawa H, Uramoto H, Onitsuka T, Chundong G, Hanagiri T, Oyama T, Yasumoto K (2011) Overexpression of MACC1 mRNA in lung adenocarcinoma is associated with postoperative recurrence. J Thorac Cardiovasc Surg 141:895–898. https://doi.org/10.1016/j.jtcvs.2010.09.044

29. Isella C, Mellano A, Galimi F, Petti C, Capussotti L, De Simone M, Bertotti A, Medico E, Muratore A (2013) MACC1 mRNA Levels Predict Cancer Recurrence After Resection of Colorectal Cancer Liver Metastases. Ann Surg 257:1089–1095. https://doi.org/10.1097/SLA.0b013e31828f96bc

30. Gao S, Lin B-Y, Yang Z, Zheng Z-Y, Liu Z-K, Wu L-M, Xie H-Y, Zhou L, Zheng S-S (2014) Role of overexpression of MACC1 and/or FAK in predicting prognosis of hepatocellular carcinoma after liver transplantation. Int J Med Sci 11:268–275. https://doi.org/10.7150/ijms.7769

31. Wang G, Fu Z, Li D (2015) MACC1 overexpression and survival in solid tumors : a meta-analysis. 1055–1065. https://doi.org/10.1007/s13277-014-2736-9

32. Stein U, Walther W, Arlt F, Schwabe H, Smith J, Fichtner I, Birchmeier W, Schlag PM (2009) MACC1, a newly identified key regulator of HGF-MET signaling, predicts colon cancer metastasis. Nat Med 15:59–67. https://doi.org/10.1038/nm.1889

33. Stein U, Burock S, Herrmann P, Wendler I, Niederstrasser M, Wernecke D, Schlag PM (2012) Circulating MACC1 Transcripts in Colorectal Cancer Patient Plasma Predict Metastasis and Prognosis. 7:1–10. https://doi.org/10.1371/journal.pone.0049249

34. Östman A, Hellberg C, Böhmer FD (2006) Protein-tyrosine phosphatases and cancer. Nat Rev Cancer 6:307–320. https://doi.org/10.1038/nrc1837

35. Ren B, Zakharov V, Yang Q, McMahon L, Yu J, Cao W (2013) MACC1 Is Related to Colorectal Cancer Initiation and Early-Stage Invasive Growth. Am J Clin Pathol 140:701–707. https://doi.org/10.1309/AJCPRH1H5RWWSXRB

36. Lemos C, Hardt MS, Juneja M, Voss C, Susann F, Jerchow B, Haider W, Bl H, Stein U (2016) MACC1 Induces Tumor Progression in Transgenic Mice and Colorectal Cancer Patients via Increased Pluripotency Markers Nanog and Oct4. 22:2812–2825. https://doi.org/10.1158/1078-0432.CCR-15-1425

37. Noh KH, Kim BW, Song K-H, Cho H, Lee Y-H, Kim JH, Chung J-Y, Kim J-H, Hewitt SM, Seong S-Y, Mao C-P, Wu T-C, Kim TW (2012) Nanog signaling in cancer promotes stem-like phenotype and immune evasion. J Clin Invest 122:4077–4093. https://doi.org/10.1172/JCI64057

38. Mohiuddin IS, Wei S-J, Kang MH (2020) Role of OCT4 in cancer stem-like cells and chemotherapy resistance. Biochim Biophys Acta - Mol Basis Dis 1866:165432. https://doi.org/10.1016/j.bbadis.2019.03.005

39. Villodre ES, Kipper FC, Pereira MB, Lenz G (2016) Roles of OCT4 in tumorigenesis, cancer therapy resistance and prognosis. Cancer Treat Rev 51:1–9. https://doi.org/10.1016/j.ctrv.2016.10.003

40. Herschman HR (1991) Primary Response Genes Induced by Growth Factors and Tumor Promoters. Annu Rev Biochem 60:281–319. https://doi.org/10.1146/annurev.bi.60.070191.001433

41. Bahrami S, Drabløs F (2016) Gene regulation in the immediate-early response process. Adv Biol Regul 62:37–49. https://doi.org/10.1016/j.jbior.2016.05.001

42. Gomard T, Jariel-Encontre I, Basbous J, Bossis G, Mocquet-Torcy G, Piechaczyk M (2008) Fos family protein degradation by the proteasome. Biochem Soc Trans 36:858–863. https://doi.org/10.1042/BST0360858

43. Healy S, Khan P, Davie JR (2013) Immediate early response genes and cell transformation. Pharmacol Ther 137:64–77. https://doi.org/10.1016/j.pharmthera.2012.09.001

44. Fowler T, Sen R, Roy AL (2011) Regulation of primary response genes. Mol Cell 44:348–360. https://doi.org/10.1016/j.molcel.2011.09.014

45. Lau LF, Nathans D (1985) Identification of a set of genes expressed during the G0/G1 transition of cultured mouse cells. EMBO J 4:3145–51

46. Charles CH, Simske JS, O'Brien TP, Lau LF (1990) Pip92: a short-lived, growth factor-inducible protein in BALB/c 3T3 and PC12 cells. Mol Cell Biol 10:6769–6774. https://doi.org/10.1128/MCB.10.12.6769

47. Ueda T, Kohama Y, Sakurai H (2019) IER family proteins are regulators of protein phosphatase PP2A and modulate the phosphorylation status of CDC25A. Cell Signal 55:81–89. https://doi.org/10.1016/j.cellsig.2018.12.012

48. Neeb A, Wallbaum S, Novac N, Dukovic-Schulze S, Scholl I, Schreiber C, Schlag P, Moll J, Stein U,

Sleeman JP (2012) The immediate early gene Ier2 promotes tumor cell motility and metastasis, and predicts poor survival of colorectal cancer patients. Oncogene 31:3796–3806. https://doi.org/10.1038/onc.2011.535

49. Ueda T, Kohama Y, Sakurai H (2019) IER family proteins are regulators of protein phosphatase PP2A and modulate the phosphorylation status of CDC25A. Cell Signal 55:81–89. https://doi.org/10.1016/j.cellsig.2018.12.012

50. Shen T, Huang S (2012) The Role of Cdc25A in the Regulation of Cell Proliferation and Apoptosis. Anticancer Agents Med Chem 12:631–639. https://doi.org/10.2174/187152012800617678

51. Xu Z, Zhu L, Wu W, Liao Y, Zhang W, Deng Z, Shen J, Yuan Q, Zheng L, Zhang Y, Shen W (2017) Immediate early response protein 2 regulates hepatocellular carcinoma cell adhesion and motility via integrin β1-mediated signaling pathway. Oncol Rep 37:259–272. https://doi.org/10.3892/or.2016.5215

52. Crosara-Alberto DP, Inoue RY, Costa CRC (2009) FAK signalling mediates NF-κB activation by mechanical stress in cardiac myocytes. Clin Chim Acta 403:81–86. https://doi.org/10.1016/j.cca.2009.01.023

53. Kyjacova L, Saup R, Rönsch K, Wallbaum S, Dukowic-schulze S, Foss A, Scherer SD, Rothley M, Neeb A, Grau N, Thiele W, Thaler S, Cremers N (2021) IER2-induced senescence drives melanoma invasion through osteopontin. Oncogene. https://doi.org/10.1038/s41388-021-02027-6

54. Ilm K, Kemmner W, Osterland M, Burock S, Koch G, Herrmann P, Schlag PM, Stein U (2015) High MACC1 expression in combination with mutated KRAS G13 indicates poor survival of colorectal cancer patients. Mol Cancer 14:1–7. https://doi.org/10.1186/s12943-015-0316-2

55. Dahlmann M, Monks A, Harris ED, Kobelt D, Osterland M, Khaireddine F, Herrmann P, Kemmner W, Burock S, Walther W, Shoemaker RH, Stein U (2022) Combination of wnt/β-catenin targets S100A4 and DKK1 improves prognosis of human colorectal cancer. Cancers (Basel) 14:. https://doi.org/10.3390/cancers14010037

56. Tsukamoto S, Ishikawa T, Iida S, Ishiguro M, Mogushi K, Mizushima H, Uetake H, Tanaka H, Sugihara K (2011) Clinical significance of osteoprotegerin expression in human colorectal cancer. Clin Cancer Res 17:2444–50. https://doi.org/10.1158/1078-0432.CCR-10-2884

57. Szklarczyk D, Gable AL, Lyon D, Junge A, Wyder S, Huerta-Cepas J, Simonovic M, Doncheva NT, Morris JH, Bork P, Jensen LJ, Mering C von (2019) STRING v11: protein–protein association networks with increased coverage, supporting functional discovery in genome-wide experimental datasets. Nucleic Acids Res 47:D607–D613. https://doi.org/10.1093/nar/gky1131

58. Stein U, Dahlmann M, Walther W (2010) MACC1 — more than metastasis? Facts and predictions about a novel gene. J Mol Med 88:11–18. https://doi.org/10.1007/s00109-009-0537-1

59. Yu W, Hurley J, Roberts D, Chakrabortty SK, Enderle D, Noerholm M, Breakefield XO, Skog JK (2021) Exosome-based liquid biopsies in cancer: opportunities and challenges. Ann Oncol 32:466–477. https://doi.org/10.1016/j.annonc.2021.01.074

60. Schneider A, Fischer A, Weber D, von Ahsen O, Scheek S, Krüger C, Rossner M, Klaussner B, Faucheron N, Kammandel B, Goetz B, Herrmann O, Bach A, Schwaninger M (2004) Restriction-mediated Differential Display (RMDD) Identifies pip92 as a Pro-Apoptotic Gene Product Induced during Focal Cerebral Ischemia. J Cereb Blood Flow Metab 24:224–236. https://doi.org/10.1097/01.WCB.0000104960.26014.7A

61. Chung KC, Sung JY, Ahn W, Rhim H, Oh TH, Lee MG, Ahn YS (2001) Intracellular Calcium Mobilization Induces Immediate Early Gene pip92 via Src and Mitogen-activated Protein Kinase in

Immortalized Hippocampal Cells. J Biol Chem 276:2132–2138. https://doi.org/10.1074/jbc.M007492200

62. Takaya T, Kasatani K, Noguchi S, Nikawa JI (2009) Functional analyses of immediate early gene ETR101 expressed in yeast. Biosci Biotechnol Biochem 73:1653–1660. https://doi.org/10.1271/bbb.90162

63. Kumar M, Gouw M, Michael S, Sámano-Sánchez H, Pancsa R, Glavina J, Diakogianni A, Valverde JA, Bukirova D, Čalyševa J, Palopoli N, Davey NE, Chemes LB, Gibson TJ (2020) ELM-the eukaryotic linear motif resource in 2020. Nucleic Acids Res 48:D296–D306. https://doi.org/10.1093/nar/gkz1030

64. Gendelman R, Xing H, Mirzoeva OK, Sarde P, Curtis C, Feiler HS, McDonagh P, Gray JW, Khalil I, Korn WM (2017) Bayesian network inference modeling identifies TRIB1 as a novel regulator of cell-cycle progression and survival in cancer cells. Cancer Res 77:1575–1585. https://doi.org/10.1158/0008-5472.CAN-16-0512

65. Chen M-S, Ryan CE, Piwnica-Worms H (2003) Chk1 Kinase Negatively Regulates Mitotic Function of Cdc25A Phosphatase through 14-3-3 Binding. Mol Cell Biol 23:7488–7497. https://doi.org/10.1128/mcb.23.21.7488-7497.2003

66. Kiely M, Kiely PA (2015) PP2A: The wolf in sheep's clothing? Cancers (Basel) 7:648–669. https://doi.org/10.3390/cancers7020648

67. Ugi S, Imamura T, Maegawa H, Egawa K, Yoshizaki T, Shi K, Obata T, Ebina Y, Kashiwagi A, Olefsky JM (2004) Protein Phosphatase 2A Negatively Regulates Insulin's Metabolic Signaling Pathway by Inhibiting Akt (Protein Kinase B) Activity in 3T3-L1 Adipocytes. Mol Cell Biol 24:8778–8789. https://doi.org/10.1128/MCB.24.19.8778-8789.2004

68. Ugi S, Imamura T, Ricketts W, Olefsky JM (2002) Protein Phosphatase 2A Forms a Molecular Complex with Shc and Regulates Shc Tyrosine Phosphorylation and Downstream Mitogenic Signaling. Mol Cell Biol 22:2375–2387. https://doi.org/10.1128/mcb.22.7.2375-2387.2002

69. Kauko O, Westermarck J (2018) Non-genomic mechanisms of protein phosphatase 2A (PP2A) regulation in cancer. Int J Biochem Cell Biol 96:157–164. https://doi.org/10.1016/j.biocel.2018.01.005

70. Kuo YC, Huang KY, Yang CH, Yang YS, Lee WY, Chiang CW (2008) Regulation of phosphorylation of Thr-308 of Akt, cell proliferation, and survival by the B55α regulatory subunit targeting of the protein phosphatase 2A holoenzyme to Akt. J Biol Chem 283:1882–1892. https://doi.org/10.1074/jbc.M709585200

71. Goh ETH, Pardo OE, Michael N, Niewiarowski A, Totty N, Volkova D, Tsaneva IR, Seckl MJ, Gout I (2010) Involvement of heterogeneous ribonucleoprotein F in the regulation of cell proliferation via the mammalian target of rapamycin/S6 kinase 2 pathway. J Biol Chem 285:17065–17076. https://doi.org/10.1074/jbc.M109.078782

72. Carpenter B, MacKay C, Alnabulsi A, MacKay M, Telfer C, Melvin WT, Murray GI (2006) The roles of heterogeneous nuclear ribonucleoproteins in tumour development and progression. Biochim Biophys Acta - Rev Cancer 1765:85–100. https://doi.org/10.1016/j.bbcan.2005.10.002

73. Stein U, Smith J, Walther W, Arlt F (2009) MACC1 controls Met: What a difference an Sp1 site makes. Cell Cycle 8:2467–2469. https://doi.org/10.4161/cc.8.15.9018

74. Birchmeier C, Birchmeier W, Gherardi E, Vande Woude GF (2003) Met, metastasis, motility and more. Nat Rev Mol Cell Biol 4:915–925. https://doi.org/10.1038/nrm1261

75. Wang L, Zhou R, Zhao Y, Dong S, Zhang J, Luo Y, Huang N, Shi M, Bin J, Liao Y, Liao W (2016) MACC-

1 Promotes Endothelium-Dependent Angiogenesis in Gastric Cancer by Activating TWIST1/VEGF-A Signal Pathway. PLoS One 11:e0157137. https://doi.org/10.1371/journal.pone.0157137

76. Celton-Morizur S, Merlen G, Couton D, Margall-Ducos G, Desdouets C (2009) The insulin/Akt pathway controls a specific cell division program that leads to generation of binucleated tetraploid liver cells in rodents. J Clin Invest 119:1880–7. https://doi.org/10.1172/jci38677

77. Zhao H, Chen Q, Alam A, Cui J, Suen KC, Soo AP, Eguchi S, Gu J, Ma D (2018) The role of osteopontin in the progression of solid organ tumour. Cell Death Dis 9:356. https://doi.org/10.1038/s41419-018-0391-6

8 STATUTORY DECLARATION

“I, Miguel Enrique Alberto Vilchez, by personally signing this document in lieu of an oath, hereby affirm that I prepared the submitted dissertation on the topic Molekulare Mechanismen des Kolorektales Karzinom: MACC1 und das neuartige IER2-Gen / Molecular mechanisms of colorectal cancer: MACC1 and the novel IER2 gene, independently and without the support of third parties, and that I used no other sources and aids than those stated.

All parts which are based on the publications or presentations of other authors, either in letter or in spirit, are specified as such in accordance with the citing guidelines. The sections on methodology (in particular regarding practical work, laboratory regulations, statistical processing) and results (in particular regarding figures, charts and tables) are exclusively my responsibility.

Furthermore, I declare that I have correctly marked all of the data, the analyses, and the conclusions generated from data obtained in collaboration with other persons, and that I have correctly marked my own contribution and the contributions of other persons (cf. declaration of contribution). I have correctly marked all texts or parts of texts that were generated in collaboration with other persons.

My contributions to any publications to this dissertation correspond to those stated in the below joint declaration made together with the supervisor. All publications created within the scope of the dissertation comply with the guidelines of the ICMJE (International Committee of Medical Journal Editors; www.icmje.org) on authorship. In addition, I declare that I shall comply with the regulations of Charité – Universitätsmedizin Berlin on ensuring good scientific practice.

I declare that I have not yet submitted this dissertation in identical or similar form to another Faculty.

The significance of this statutory declaration and the consequences of a false statutory declaration under criminal law (Sections 156, 161 of the German Criminal Code) are known to me.”

_____ _____

Date Signature

9 CURRICULUM VITAE

Mein Lebenslauf wird aus datenschutzrechtlichen Gründen in der elektronischen Version meiner Arbeit nicht veröffentlicht.

My curriculum vitae will not be published in the electronic version of my work for data protection reasons.

Mein Lebenslauf wird aus datenschutzrechtlichen Gründen in der elektronischen Version meiner Arbeit nicht veröffentlicht.

My curriculum vitae will not be published in the electronic version of my work for data protection reasons.

10 ACKNOWLEDGEMENTS

To my parents and my brother, for their unconditional emotional and financial support during the research and writing of this thesis.

To Geraldine, for not abandoning her stubborn faith in me and my abilities.

Mein besonderer Dank gilt Fr. Prof. Ulrike Stein und Fr. Prof. Beate Rau. Sie zeigten mir den Weg und bereiteten ihn vor. Danke, dass Sie mich auch mitgenommen haben.

To my colleagues, but also friends, Benedikt and Fabian, whose scientific know-how and acute constructive criticism shaped and transformed this thesis.

To my friends and dearest ones, without whose support and shoulders to bare the weight upon, would have led me to quit prematurely.

To my country and the magna Universidad Central de Venezuela, whose academic values dared me to dream bigger and bolder.

This is the first step towards a long path. I do this all for you.

CHARITÉ

CharitéCentrum für Human- und Gesundheitswissenschaften

Charité | Campus Charité Mitte | 10117 Berlin

Name, Vorname: Alberto Vílchez, Miguel Enrique
Emailadresse: miguel.alberto@charite.de
Matrikelnummer: 02248670

PromotionsbetreuerIn:
Prof. Dr. Ulrike Stein und Prof. Dr. med. Beate Rau
Promotionsinstitution / Klinik: Experimental and Clinical Research Center und Chirurgische Klinik

Institut für Biometrie und klinische Epidemiologie (iBikE)

Direktor: Prof. Dr. Geraldine Rauch

Postanschrift:
Charitéplatz 1 | 10117 Berlin
Besucheranschrift:
Reinhardtstr. 58 | 10117 Berlin

Tel. +49 (0)30 450 562171
geraldine.rauch@charite.de
https://biometrie.charite.de/

Bescheinigung

Hiermit bescheinige ich, dass Herr Miguel E. Alberto V. innerhalb der Service Unit Biometrie des Instituts für Biometrie und klinische Epidemiologie (iBikE) bei mir eine statistische Beratung zu einem Promotionsvorhaben wahrgenommen hat. Folgende Beratungstermine wurden wahrgenommen:

- Termin 1: 04.11.2021
- Termin 2: 15.12.2021

Folgende wesentliche Ratschläge hinsichtlich einer sinnvollen Auswertung und Interpretation der Daten wurden während der Beratung erteilt:

- Die Statistik entspricht den Anforderungen einer medizinischen Promotion.

Diese Bescheinigung garantiert nicht die richtige Umsetzung der in der Beratung gemachten Vorschläge, die korrekte Durchführung der empfohlenen statistischen Verfahren und die richtige Darstellung und Interpretation der Ergebnisse. Die Verantwortung hierfür obliegt allein dem Promovierenden. Das Institut für Biometrie und klinische Epidemiologie übernimmt hierfür keine Haftung.

Datum: 16.12.2021 Name des Beraters/der Beraterin: Jochen Kruppa

_____

Unterschrift BeraterIn, Institutsstempel